PHYSICAL REVIEW D **95,** 095013 (2017)

Radiative electroweak symmetry breaking in standard model extensions

K. S. Babu,[1,*] Ilia Gogoladze,[2,†] and S. Khan[1,‡]

[1]*Department of Physics, Oklahoma State University, Stillwater, Oklahoma 74078, USA*
[2]*Bartol Research Institute, Department of Physics and Astronomy, University of Delaware, Newark, Delaware 19716, USA*

(Received 2 January 2017; published 17 May 2017)

We study the possibility of radiative electroweak symmetry breaking where loop corrections to the mass parameter of the Higgs boson trigger the symmetry breaking in various extensions of the Standard Model (SM). Although the mechanism fails in the SM, it is shown to be quite successful in several extensions which share a common feature of having an additional scalar around the TeV scale. The positive Higgs mass parameter at a high energy scale is turned negative in the renormalization group flow to lower energy by the cross couplings between the scalars in the Higgs potential. The type-II seesaw model with a TeV scale weak scalar triplet, a two-loop radiative neutrino mass model with new scalars at the TeV scale, the inert doublet model, scalar singlet dark matter model, and a universal seesaw model with an additional $U(1)$ broken at the TeV scale are studied and shown to exhibit successful radiative electroweak symmetry breaking.

DOI: 10.1103/PhysRevD.95.095013

I. INTRODUCTION

Discovery of the Higgs boson as predicted by the Standard Model (SM) by the ATLAS and the CMS experiments became the moment of triumph for particle physics [1,2]. Such a historic discovery together with decades of eletroweak precision data have well established the validity of SM up to accessible energies. However, there is no verified explanation of the origin of the small neutrino masses and no viable candidate for the dark matter in the SM. Due to these unwavering issues, various extensions of SM have been proposed. The secret of neutrino masses may lie in some form of seesaw mechanism, where a SM singlet right-handed neutrino with large Majorana masses cause the light neutrino masses (type-I seesaw) [3] or a SM weak scalar triplet with a tiny induced vacuum expectation value (vev) generates the small neutrino masses (type-II seesaw) [4]. If neutrino masses are generated as loop corrections, the masses will naturally be suppressed and such extensions of SM are both theoretically well motivated and phenomenologically viable [5,6].

Searches for a stable dark matter candidate have also been motivation for various extensions of the SM. Some form of symmetry usually stabilizes the dark matter. Simple discrete symmetries such as R-parity in supersymmetric models [7] can perform an excellent job of preventing the particle from decaying. Kaluza-Klein parity [8] in universal extra dimension models and T-parity in the littlest Higgs models [9] can stabilize the lightest particle, turning them into promising dark matter candidates. A similar role is played by a $\mathbb{Z}_2$ symmetry for the case of inert doublet models [10] or scotogenic models [11]. SM extended by a scalar singlet carrying a discrete $\mathbb{Z}_2$ parity is yet another example for a simple dark matter model. Instead of being an *ad hoc* symmetry, this $\mathbb{Z}_2$ symmetry can be a remnant of the $(B-L)$ generator of $SO(10)$ grand unified theories (GUTs) [12].

$SO(10)$ GUTs provide one of the most lucrative frameworks, where one can incorporate many of the aforementioned extensions of SM along with a beautiful unified picture of SM gauge couplings. Among the classes of $SO(10)$ GUTs, supersymmetric versions have multiple features such as successful unification of gauge couplings and a natural dark matter candidate owing to an automatic R-parity, while it solves the gauge hierarchy problem based on the symmetry principle. In addition, supersymmetric models offer a mechanism for triggering electroweak symmetry breaking (EWSB) via radiative effects [13]. In this scenario, the positive mass parameter of the Higgs boson at high energy becomes negative at low energy due to the renormalization group flow which dictates how the parameters evolve with scale.

The purpose of this paper is to explore the possibility of radiative EWSB breaking in nonsupersymmetric (non-SUSY) extensions of the SM. Since this is an attractive mechanism to trigger EWSB, checking its viability in non-SUSY models is of great interest. As we argue below, such a radiative EWSB may be necessary in certain unified theories which have two stages of symmetry breaking. In a general context a positive mass parameter for the Higgs boson turning negative also enhances the available parameter space.

In some extensions of the SM, the Higgs boson is a part of the larger multiplet, which breaks some higher symmetry.

*kaladi.babu@okstate.edu
†ilia@bartol.udel.edu
‡saki.khan@okstate.edu

This occurs in trinification models based on $SU(3)_C \times SU(3)_L \times SU(3)_R$ gauge symmetry [14–16] broken by two $(1,3,3^*)$ Higgs multiplets. These multiplets contain SM singlet components which acquire large vevs breaking the gauge symmetry down to SM. The same $(1,3,3^*)$ multiplets also contain the Higgs boson of the SM which should develop a negative squared mass to trigger EWSB. Consistency of the high scale symmetry breaking, however, would demand that all physical Higgs bosons, including the SM Higgs, have positive squared masses at a high energy. One could introduce new Higgs fields to break the electroweak symmetry in which case the model loses its minimality and predictivity. For such class of models one might employ radiative loop corrections to turn the Higgs mass parameter negative at low energy from the positive value it obtained at high energy and thus cause electroweak symmetry breaking. A second example is provided by a class of $SO(10)$ models with the symmetry breaking sectors containing $\overline{126}_H$ along with either a 45_H or a 210_H [17] where flavor mixing is induced by vectorlike fermions in the $16+\overline{16}$ representation. In such models, the SM singlet from $\overline{126}_H$ acquires a GUT scale vev, breaking $SO(10)$ down to $SU(5)$. The $\overline{126}_H$ also contains a SM Higgs doublet which must have positive squared mass at the GUT scale. This positive mass term can turn negative at low energy due to renormalization group flow. Similar arguments can be applied for the case where a SM singlet of 144 representation breaks $SO(10)$ down to the SM [18]. The Higgs doublet is also part of 144, which should have a positive squared mass at the GUT scale.

In this paper we explore the possibility of radiative electroweak symmetry breaking in several popular extensions of the SM. The mechanism fails in the SM, as reviewed in Sec. II. In type-I seesaw models which includes right-handed neutrinos to the spectrum of the SM, radiative EWSB is not achieved—in fact the effect of ν_R fields is to provide *positive* corrections to the Higgs mass parameter in evolving from high to low energies. The situation is different in type-II seesaw models which contain a weak scalar triplet, if the mass of the triplet is around the TeV scale. The key difference is the cross coupling between the SM Higgs boson and an additional scalar field in the Higgs potential. The need for this additional scalar field to be at the TeV scale arises from the needed magnitude of the μ_ϕ^2 parameter: $\mu_\phi^2 = -(88\ \text{GeV})^2$. As the correction to μ_ϕ^2 from the scalar cross coupling grows as $-(m_\Delta^2)$ of the new scalar, this scalar should not be much heavier than a TeV, assuming that the quartic cross couplings are not extremely weak.

Radiative mass generation is a popular mechanism for neutrino masses where one assumes new scalars at the TeV scale for lepton number violation. Such models are amenable to radiative EWSB. Dark matter models employing a scalar singlet or an inert doublet also exhibit radiative EWSB. Finally, we propose and analyze a universal seesaw model wherein a new $U(1)$ symmetry is broken at the TeV scale, which also shows radiative EWSB.

In nonsupersymmtric extensions of the SM such as the ones studied here, the gauge hierarchy problem has to be somehow solved. One may address the issue by introducing a classically scale invariant theory [19]. Here we simply assume that this is done by fine-tuning. The dimensionful parameters of the SM extensions are given by

$$\mathcal{L}_{\text{SM}} = \Lambda_{\text{cos}}^4 + \Lambda^2 \mu_\phi^2 + \cdots \tag{1.1}$$

where the $\cdots$ donate mass parameters for additional scalar fields that may be present and Λ_{cos} is the cosmological constant. These dimensionful parameters may take, for reasons not understood, special values, rather than their "natural values" which are of order the Planck scale. Once the scalar masses are set at these special (or fine-tuned) values, we assume that the corrections to μ_ϕ^2 arising from other particles present in the model do not exceed the physical mass of ϕ.

A positive mass parameter turning negative via renormalization group equation (RGE) flow leads to dimensional transmutation as can be seen in a Coleman-Weinberg [20] analysis of the effective potential. The RGE evolution that we employ is in one-to-one correspondence with the effective potential, where the minimization is performed at a momentum scale close to the mass of the Higgs scalar.

The outline of the paper is as follows. In Sec. II, we discuss the absence of such radiative EWSB in the SM and type-I seesaw model. Even though such a mechanism fails for type-I seesaw models, in Sec. III we show that the presence of a TeV scale weak triplet makes radiative EWSB a success for the case of type-II seesaw models. In Sec. IV, we show that for a two-loop neutrino mass model positive Higgs mass parameter at a high energy scale turns negative in the renormalization group flow to low energy. In Secs. V and VI, we show that simple dark matter models such as the inert doublet model and the scalar singlet dark matter model also exhibit radiative EWSB when the models have TeV scale scalar(s) coupled to the SM Higgs boson. In Sec. VII, we study the radiative EWSB for a universal seesaw model. Finally in Sec. VIII we conclude.

II. ABSENCE OF RADIATIVE EWSB IN SM AND TYPE-I SEESAW MODELS

The mechanism of radiative EWSB occurs when the renormalization group flow of the Higgs mass parameter (μ_ϕ^2) receives enough negative contribution from various parameters of the model turning the positive quantity into a negative one while evolving from high to low energies. Unfortunately such cannot be the case in the SM.

The Higgs potential of the SM is given by

$$V(\phi) = \mu_\phi^2 \phi^\dagger \phi + \frac{\lambda}{2}(\phi^\dagger \phi)^2.$$

And the RGE of mass parameter (μ_ϕ^2) is given by [21]

$$16\pi^2 \frac{d\mu_\phi^2}{dt} = \mu_\phi^2 \left(6\lambda + 2\mathrm{Tr}(3\mathbf{Y_u^\dagger Y_u} + 3\mathbf{Y_d^\dagger Y_d} + 3\mathbf{Y_e^\dagger Y_e}) - \frac{9}{10} g_1^2 - \frac{9}{2} g_2^2 \right).$$

The evolution of the Higgs mass parameter (μ_ϕ^2) is dominated by the gauge couplings and the top quark Yukawa couplings. However, these corrections are proportional to μ_ϕ^2 itself, which implies that a positive μ_ϕ^2 cannot turn into negative μ_ϕ^2 in RGE evolution making radiative EWSB an impossibility within SM.

For type-I seesaw models, the additional Lagrangian is given by

$$\mathcal{L} \supset -(\mathbf{Y_\nu})_{ij} v \overline{\nu_R}^i \nu_L^j - (\mathbf{M_R})_{ij} \overline{\nu_R}^i \mathrm{C} \nu_R^j.$$

This part of the Lagrangian manages to contribute in the renormalization group flow as it adds a new term to the RGE of Higgs mass parameter:

$$16\pi^2 \frac{d\mu_\phi^2}{dt} = 16\pi^2 \left(\frac{d\mu_\phi^2}{dt} \right)_{\mathrm{SM}} - 4\mathrm{Tr}(\mathbf{Y}_\nu \mathbf{Y}_\nu^\dagger \mathbf{M_R^\dagger M_R})$$

Unfortunately, the contributions coming from the ν_R fields make the situation worse as they only strengthen the positivity of the mass parameter as it evolves from high to low energies. One should also notice that if we want to use the criterion of naturalness, i.e. the correction to the Higgs mass parameter $\lesssim 1$ TeV^2, the scale of the Majorana mass of the right-handed neutrino should not exceed 7.4×10^7 GeV [22].

In supersymmetry, the radiative EWSB becomes successful [13] as the scalar partners of the fermions contribute significantly in the renormalization group flow of the Higgs mass parameter in the right direction, making the positive term negative as it evolves from high to low energies. Similar incidents occur in other extensions of SM such as type-II seesaw models where the TeV scale particle(s) manages to dominate the renormalization group flow and turn the positive value of the Higgs mass parameter into negative value triggering radiative EWSB. A common feature of these extensions is the presence of new scalar(s) at the TeV scale as we show in the next five sections.

III. RADIATIVE EWSB IN A TYPE-II SEESAW NEUTRINO MASS MODEL

While the type-I seesaw model needs right-handed (RH) neutrinos which are neutral under the Standard Model gauge group with large Majorana masses, the minimal type-II seesaw mechanism requires the existence of a weak scalar triplet. The most natural source for such triplets is provided by the left-right symmetric theories which can be realized either at low energy or can be embedded in grand unified theories such as $SO(10)$ or E_6. Here we study the potential radiative EWSB scenario of the type-II seesaw extension of the SM.

A. The model

We consider the possibility that the weak scalar triplet $\Delta(1,3,1)$ is the only low-energy remnant of the new physics beyond the SM and the neutral component (Δ^0) acquires a very small induced vev at low energy. The SM electroweak doublet $\phi(1,2,\frac{1}{2})$ and the electroweak triplet $\Delta(1,3,1)$ are denoted by

$$\phi = \begin{pmatrix} \phi^+ \\ \phi^0 \end{pmatrix}; \qquad \Delta = \frac{\sigma_i}{\sqrt{2}} \Delta_i = \begin{pmatrix} \frac{\Delta^+}{\sqrt{2}} & \Delta^{++} \\ \Delta^0 & \frac{\Delta^+}{\sqrt{2}} \end{pmatrix} \tag{3.1}$$

where σ_i's are the Pauli matrices. The most general renormalizable tree-level scalar potential is

$$\begin{aligned} V(\phi,\Delta) = {} & \mu_\phi^2 \phi^\dagger \phi + \frac{\lambda_1}{2}(\phi^\dagger \phi)^2 + \mu_\Delta^2 \mathrm{Tr}(\Delta^\dagger \Delta) \\ & + \frac{\lambda_2}{2}(\mathrm{Tr}(\Delta^\dagger \Delta))^2 + \frac{\lambda_3}{2}[(\mathrm{Tr}(\Delta^\dagger \Delta))^2 \\ & - \mathrm{Tr}(\Delta^\dagger \Delta \Delta^\dagger \Delta)] + \lambda_4 \phi^\dagger \phi \mathrm{Tr}(\Delta^\dagger \Delta) \\ & + \lambda_5 \phi^\dagger [\Delta^\dagger, \Delta] \phi + \left\{ \frac{\mu}{\sqrt{2}} \phi^T i\sigma_2 \Delta^\dagger \phi + \mathrm{H.c.} \right\}. \end{aligned} \tag{3.2}$$

The weak triplet also generates a Majorana mass term for the neutrinos through the Yukawa Lagrangian (corresponding Feynman diagram given in Fig. 1):

$$\mathcal{L}_Y \supset -\frac{(\mathbf{Y}_\Delta)_{ij}}{\sqrt{2}} \ell_i^T C i\sigma_2 \Delta \ell_j + \mathrm{H.c.} \tag{3.3}$$

With the vev of the electroweak doublet $\langle \phi \rangle = v$, an effective dimension 5 operator generates the neutrino masses through the small but nonzero induced VEV, $\langle \Delta \rangle = \frac{\mu v^2}{\sqrt{2}\mu_\Delta^2} \ll v$ when $v \ll \mu_\Delta$ and/or μ is so small that $\mu v^2 \ll \mu_\Delta^2$ as the electroweak triplet decouples. The neutrino mass matrix is given by

$$\mathbf{m}_\nu \simeq \mathbf{Y}_\Delta \frac{\mu v^2}{2\mu_\Delta^2}. \tag{3.4}$$

Here one assumes $\mu_\Delta^2 > 0$ so that $\langle\Delta\rangle$ is induced only after $\langle\phi\rangle = v$ is generated.

One also needs to realize the fact that integrating out the heavy scalar triplet in the tree-level approximation will also have an effect on the SM Higgs quartic coupling. The effective quartic coupling below the scale $\mu_r = \mu_\Delta$ is given by

$$\lambda_1^{\rm eff} = \lambda_1 - \frac{\mu^2}{\mu_\Delta^2}. \tag{3.5}$$

This is the connecting formula for the Standard Model quartic coupling λ_1 at the scale $\mu_r = \mu_\Delta$.

B. The stability conditions for the Higgs potential and the evolution of mass parameters

One needs to be careful while studying the solution to the set of RGEs of the parameters of a model. The parameters in the scalar potential have to satisfy certain conditions at all energy scales which ensures that the potential is bounded from below. For that purpose one must identify the necessary and sufficient conditions for boundedness of the potential. For type-II seesaw models, the stability conditions for the potential to be bounded from below can be derived to be

$$\text{(i)}\quad \lambda_1 \geq 0; \qquad \lambda_2 \geq 0; \tag{3.6}$$

$$\text{(ii)}\quad \lambda_4 - |\lambda_5| \geq -\sqrt{\lambda_1\lambda_2}; \qquad 2\lambda_2 + \lambda_3 \geq 0; \tag{3.7}$$

$$\text{(iii)}\quad 2\lambda_4\sqrt{\lambda_2} + 2\lambda_2\sqrt{\lambda_1} + \lambda_3\sqrt{\lambda_1} \geq 0 \quad \text{or,}$$
$$-2\lambda_1\lambda_2\lambda_3 - \lambda_1\lambda_3^2 + 2\lambda_3\lambda_4^2 - 2(2\lambda_2 + \lambda_3)\lambda_5^2 \geq 0. \tag{3.8}$$

This is a compact set of constraints that is necessary and sufficient as we show in Appendix A. For a less compact set of constraints see Ref. [23]. The couplings of the Lagrangian have to maintain these stability conditions up to the energy scale of new physics such as GUTs.

Using vertex corrections and the wave function renormalization factors, we can calculate the complete set of

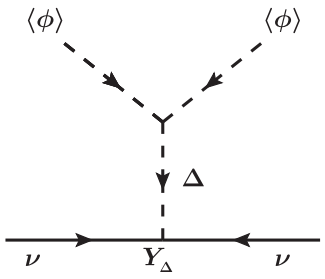

FIG. 1. Diagrammatic representation of type-II seesaw.

TABLE I. Quartic couplings and mass parameter values for the sample point used for the type-II seesaw model in Fig. 2.

Quartic couplings	Values	Mass parameters	Values
$\lambda_1(m_Z)$	0.258	$m_t(m_t)$	162.25 GeV
$\lambda_1(\mu_\Delta)$	0.1887	$\mu_\Delta^2(\mu_\Delta)$	500^2 $(\text{GeV})^2$
$\lambda_2(\mu_\Delta)$	0.15	$v(m_Z)$	174.10 GeV
$\lambda_3(\mu_\Delta)$	0.45	$\mu_\phi^2(125\ \text{GeV})$	$-(88.91)^2$ $(\text{GeV})^2$
$\lambda_4(\mu_\Delta)$	0.19	$\mu_\phi^2(\mu_\Delta)$	$-(89.59)^2$ $(\text{GeV})^2$
$\lambda_5(\mu_\Delta)$	0.10	$\mu(\mu_\Delta)$	10^{-5} GeV

β-functions and renormalization group equations. We have also determined the RGEs for the mass parameters of the model which are related to the anomalous dimensions (γ_m) of the scalar masses by

$$\gamma_m \equiv \frac{1}{2}\frac{d\ln(m^2)}{dt} \tag{3.9}$$

where $t = \ln\mu_r$ and μ_r is the running scale. The set of RGEs for the mass parameters is given by[1]

$$\begin{aligned}
16\pi^2\frac{d\mu_\phi^2}{dt} &= \left[-\frac{9}{10}g_1^2 - \frac{9}{2}g_2^2 + 6\lambda_1 + 2T\right]\mu_\phi^2 \\
&\quad + 6\lambda_4\mu_\Delta^2 + 6|\mu|^2; \\
16\pi^2\frac{d\mu_\Delta^2}{dt} &= \left[\left(-\frac{18}{5}g_1^2 - 12g_2^2\right) + 8\lambda_2 + 2\lambda_3\right. \\
&\quad \left. + 2\text{Tr}(\mathbf{Y_\Delta^\dagger Y_\Delta})\right]\mu_\Delta^2 + 4\lambda_4\mu_\phi^2 + 2|\mu|^2; \\
16\pi^2\frac{d\mu}{dt} &= \left[\lambda_1 + 4\lambda_4 - 8\lambda_5 - \frac{27}{10}g_1^2 - \frac{21}{2}g_2^2\right. \\
&\quad \left. + 2T + \text{Tr}(\mathbf{Y_\Delta^\dagger Y_\Delta})\right]\mu;
\end{aligned} \tag{3.10}$$

where

$$T = \text{Tr}[\mathbf{Y_e^\dagger Y_e} + 3\mathbf{Y_d^\dagger Y_d} + 3\mathbf{Y_u^\dagger Y_u}]. \tag{3.11}$$

A complete set of RGEs for all the couplings of the Lagrangian is given in the Appendix B. With this set of RGEs we proceed towards its numerical solution. We can already see that the contribution from the cubic coupling μ and quartic couplings such as λ_4 has the potential to drive

[1]We disagree with the signs of terms involving the couplings λ_4 and λ_5 in the RGE of the mass parameter μ given in Eq. (17) of Ref. [24]. We also disagree with the coefficient in front of the mass parameter $|\mu|$ in the RGE of μ_Δ^2 given in Eq. (18) of Ref. [24].

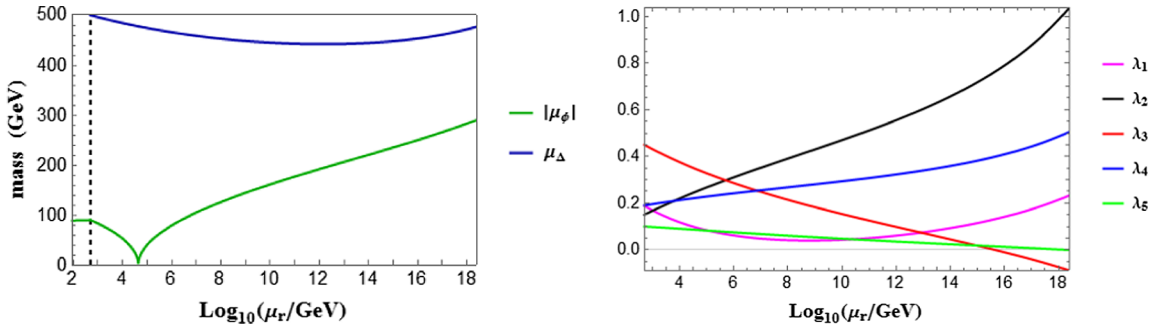

(a) Evolution of mass parameters

(b) Evolution of quartic couplings

FIG. 2. One-loop running of the parameters of type-II seesaw model from Planck scale down to weak scale. The black dashed line in (a) corresponds to the scale, $\mu_r = \mu_\Delta$. In (a) the evolution of the absolute value of the SM Higgs mass parameter ($|\mu_\phi|$) along with the mass of the weak triplet scalar (μ_Δ) has been plotted. The point at which $|\mu_\phi|$ touches the horizontal axis corresponding to mass = 0 GeV is the energy scale where radiative EWSB is triggered as the sign of the SM Higgs mass-squared parameter (μ_ϕ^2) switches from positive to negative while evolving from high to low energies. Note that in this sample case, the radiative EWSB is prompted at around an energy scale of 30 TeV. Figure 2(b) shows the evolution of all the quartic couplings of the type-II seesaw model from Planck scale down to weak scale emphasizing the fact that the model remains perturbative all the way for the selected sample point.

the positive mass parameter μ_ϕ^2 at high energy scale towards a negative value at lower energy scale to trigger radiative EWSB. For a TeV scale scalar triplet mass one realizes that to get the correct order of neutrino mass, the cubic parameter μ needs to be very small ($\sim 10^{-5}$ GeV), which makes the contribution of the μ term in the RGEs of mass parameters irrelevant. This choice is natural, since quantum corrections to μ are proportional to μ itself; see Eq. (3.10).

One can expand the procedure and calculate the two-loop corrections to the Higgs mass for the type-II seesaw model [25]. Such corrections will always depend on the mass of the Higgs triplet (μ_Δ). As the newly introduced triplet mass is near or below the TeV scale, such corrections will keep the Higgs bosons around TeV scale even at a high energy scale and will neither spoil the radiative electroweak symmetry breaking mechanism nor provide any new contribution to the hierarchy problem that has been discussed earlier (in Sec. I). So, even though such corrections may update the numerical value of the sample point of the model determined in the next section (see Sec. III C) as any higher loop correction does, such subleading corrections were avoided for the sake of simplicity. One should also note that this discussion and conclusion about a two-loop correction of the Higgs mass is applicable to all the models considered in this paper.

C. Solution to the RGEs

To analyze the evolution of the mass parameters, one needs to solve the set of RGEs which in turn requires one to define the relevant couplings at some energy scale [26]. In this case, all the SM gauge couplings, Yukawa couplings, and Higgs quartic couplings were evaluated at two-loop level up to the energy scale corresponding to the scalar triplet mass. At energies above the triplet mass, the gauge couplings were evolved continuously but with the updated RGEs given in the set of RGEs in Eq. (B3). The quartic coupling of the SM electroweak doublet Higgs has a discontinuity at the triplet mass scale due to the matching condition of the parameter given in Eq. (3.5). Above the energy scale μ_Δ, the full set of RGEs was used to evolve all the parameters of the model.

To generate a sample case, we specified the values of the quartic couplings and mass parameters of the model at the low energy scale, $\mu_r = \mu_\Delta$, consistent with the stability conditions given in the inequalities Eqs. (3.6), (3.7), and (3.8). Also the masses of neutrinos put a natural limit on the cubic coupling of the model because of Eq. (3.4) and this in turn makes the discontinuity in the Higgs quartic coupling λ_1 ignorable. To illustrate the phenomenon of radiative electroweak symmetry breaking in the type-II seesaw model, a sample point is chosen as given in Table I. The sample point satisfies all the stability conditions and the mass parameter μ_ϕ^2 runs with a positive slope with the energy scale. Figure 2 shows that the mass parameter becomes negative at low energy even though it is positive at high energy scale. This turning occurs at $\mu_r \approx 10^5$ GeV, when $|\mu_\phi|$ plotted in Fig. 2(a) becomes zero. This analysis shows that radiative electroweak symmetry breaking may be successfully achieved in type-II seesaw models. The mass of the triplet scalar should remain below about a few TeV or else μ_ϕ^2 becomes too negative.

IV. RADIATIVE EWSB IN A TWO-LOOP NEUTRINO MASS MODEL

Even before the experimental discovery of neutrino oscillation which is a clear indication of nonzero neutrino masses and mixings, the subject of neutrino mass

generation has been an active arena of research. An interesting alternative to the type-I or type-II seesaw mechanism is that the neutrino masses are generated by loop corrections, hence the masses are suppressed by the loop factors. In this scenario, the new particles responsible for the neutrino mass generation should be relatively light with the possibility that they show up at the Large Hadron Collider in the near future.

A. The Model

We will consider the two-loop neutrino mass model which introduces a doubly charged (k^{++}) and a singly charged (h^+) scalar along with the SM particles [6,27]. In this model, the lepton number is explicitly broken and as a result a tiny Majorana mass arises through the loop diagram at the two-loop level. One of the salient features of the model is that one of the three neutrino masses is very nearly zero. The model admits both normal and inverted hierarchy of neutrino masses and also has CP violation in neutrino oscillations.

The new scalars under the SM gauge group $SU(3)_C \times SU(2)_L \times U(1)_Y$ are denoted by

$$h^+(1,1,1); \qquad k^{++}(1,1,2). \tag{4.1}$$

The gauge invariant Yukawa couplings that are allowed involving the new scalars are

$$\mathcal{L}_Y \supset \mathbf{f}_{ab}\ell^i_a\ell^j_b\epsilon_{ij}h^+ + \mathbf{h}_{ab}e^c_a e^c_b k^{--} + \text{H.c.} \tag{4.2}$$

Here a, b are generation indices, i, j are $SU(2)_L$ indices with ϵ_{ij} being the antisymmetric tensor. The Yukawa coupling matrices $\mathbf{f}$ and $\mathbf{h}$ are antisymmetric and symmetric, respectively.

The scalar potential for the model is given by

$$\begin{aligned} V(\phi,h^+,k^{++}) = {} & \mu_\phi^2\phi^\dagger\phi + \mu_h^2 h^+h^- + \mu_k^2 k^{++}k^{--} \\ & - (\mu h^+h^+k^{--} + \text{H.c.}) + \frac{\lambda_1}{2}(\phi^\dagger\phi)^2 \\ & + \frac{\lambda_2}{2}(h^+h^-)^2 + \frac{\lambda_3}{2}(k^{++}k^{--})^2 \\ & + \lambda_4(\phi^\dagger\phi)(h^+h^-) + \lambda_5(\phi^\dagger\phi)(k^{++}k^{--}) \\ & + \lambda_6(h^+h^-)(k^{++}k^{--}). \end{aligned} \tag{4.3}$$

Small neutrino mass matrix is generated by a two-loop process involving the couplings $\mathbf{f}$, $\mathbf{h}$ and μ—the simultaneous presence of these couplings break lepton number—depicted in the Feynman diagram shown in Fig. 3. Neutrino oscillation phenomenology of this model has been studied extensively [27–29]. Our goal here is to study the renormalization group flow of the Higgs mass parameter and determine the possibility of radiative EWSB. While performing such a study, one also needs to be certain that the scalar potential of the model remains bounded and also that the model remains perturbative.

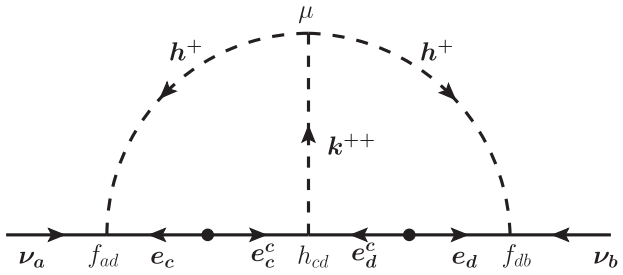

FIG. 3. Feynman Diagram responsible for neutrino mass generation at the two-loop level.

B. The stability conditions for the Higgs potential and the evolution of mass parameters

The necessary and sufficient boundedness conditions for the Higgs potential which ensures that the potential is bounded from below are given by [27]

$$\begin{aligned} &\text{(i) } \lambda_1 \geq 0; \qquad \lambda_2 \geq 0; \qquad \lambda_3 \geq 0; \\ &\text{(ii) } \lambda_4 \geq -\sqrt{\lambda_1\lambda_2}; \qquad \lambda_5 \geq -\sqrt{\lambda_1\lambda_3}; \qquad \lambda_6 \geq -\sqrt{\lambda_2\lambda_3}; \\ &\text{(iii) } \lambda_4\sqrt{\lambda_3} + \lambda_6\sqrt{\lambda_1} + \lambda_5\sqrt{\lambda_2} + \sqrt{\lambda_1\lambda_2\lambda_3} \geq 0 \quad \text{or} \\ &\quad \det\boldsymbol{\lambda} \geq 0; \end{aligned} \tag{4.4}$$

where

$$\boldsymbol{\lambda} = \begin{pmatrix} \lambda_1 & \lambda_4 & \lambda_5 \\ \lambda_4 & \lambda_2 & \lambda_6 \\ \lambda_5 & \lambda_6 & \lambda_3 \end{pmatrix}. \tag{4.5}$$

It has been shown that the model maintains perturbativity all the way to the Planck scale and boundedness for both the normal and inverted case, if $|\mathbf{h}_{\mu\mu}| < 0.45$ and $|\mathbf{f}_{\mu\tau}| < 0.34$ [27]. For the antisymmetric Yukawa coupling matrix $\mathbf{f}$, the neutrino mixing angles provide two constraints, reducing the number of free parameters to one. For the case of normal neutrino mass hierarchy the relation is given by [28]

$$\begin{aligned} \epsilon &= \tan\theta_{12}\frac{\cos\theta_{23}}{\cos\theta_{13}} + \tan\theta_{13}\sin\theta_{23}e^{-i\delta}; \\ \epsilon' &= \tan\theta_{12}\frac{\sin\theta_{23}}{\cos\theta_{13}} - \tan\theta_{13}\cos\theta_{23}e^{-i\delta}. \end{aligned} \tag{4.6}$$

And for the inverted mass hierarchy we have

TABLE II. Quartic and Yukawa coupling and mass parameter values for the sample point used for the two-loop neutrino mass model in Fig. 4.

Quartic, Yukawa couplings	Values	Mass paramters	Values
$\lambda_1(M_Z)$	0.258	$m_t(m_t)$	162.25 GeV
$\lambda_1(\mu_0)$	0.1924	$M_h(m_Z)$	125.1 GeV
$\lambda_2(\mu_0)$	0.20	$v(m_Z)$	174.10 GeV
$\lambda_3(\mu_0)$	0.50	$\mu(\mu_0)$	500 GeV
$\lambda_4(\mu_0)$	0.10	$\mu_h^2(\mu_0)$	800^2 $(\text{GeV})^2$
$\lambda_5(\mu_0)$	0.15	$\mu_k^2(\mu_0)$	450^2 $(\text{GeV})^2$
$\lambda_6(\mu_0)$	−0.25	$\mu_\phi^2(125\ \text{GeV})$	$-(88.91)^2$ $(\text{GeV})^2$
$\lvert\mathbf{f}_{\mu\tau}\rvert(\mu_0)$	0.013	$\mu_\phi^2(\mu_0)$	$-(89.55)^2$ $(\text{GeV})^2$
$\lvert\mathbf{h}_{\mu\mu}\rvert(\mu_0)$	0.4		

$$\epsilon = -\sin\theta_{23}\cot\theta_{13}e^{-i\delta}; \qquad \epsilon' = \cos\theta_{23}\cot\theta_{13}e^{-i\delta}, \tag{4.7}$$

where in both case ϵ and ϵ' are defined as

$$\epsilon \equiv \frac{\mathbf{f}_{e\tau}}{\mathbf{f}_{\mu\tau}}; \qquad \epsilon' \equiv \frac{\mathbf{f}_{e\mu}}{\mathbf{f}_{\mu\tau}}. \tag{4.8}$$

Similar to the analysis of the type-II seesaw model in Sec. III, we require the full set of RGEs for this model which includes the evolution of the gauge couplings, Yukawa couplings, quartic couplings, and the mass parameters of the Lagrangian. While the complete set of the RGEs is listed in Appendix C, the RGEs for the mass parameters of the Lagrangian are given by

$$\begin{aligned}
16\pi^2\frac{d\mu_\phi^2}{dt} &= \mu_\phi^2\left(-\frac{9}{10}g_1^2-\frac{9}{2}g_2^2+2T+6\lambda_1\right)\\
&\quad+2\lambda_4\mu_h^2+2\lambda_5\mu_k^2;\\
16\pi^2\frac{d\mu_h^2}{dt} &= \mu_h^2\left(-\frac{18}{5}g_1^2+8\mathrm{Tr}(\mathbf{f}^\dagger\mathbf{f})+4\lambda_2\right)\\
&\quad+4\lambda_4\mu_\phi^2+2\lambda_6\mu_k^2+8\mu^2;\\
16\pi^2\frac{d\mu_k^2}{dt} &= \mu_k^2\left(-\frac{72}{5}g_1^2+4\mathrm{Tr}(\mathbf{h}^\dagger\mathbf{h})+4\lambda_3\right)\\
&\quad+4\lambda_5\mu_\phi^2+2\lambda_6\mu_h^2+4\mu^2;\\
16\pi^2\frac{d\mu}{dt} &= \mu\left(-\frac{54}{5}g_1^2+2\lambda_2+2\lambda_6\right.\\
&\quad\left.+2\mathrm{Tr}(\mathbf{h}^\dagger\mathbf{h})+8\mathrm{Tr}(\mathbf{f}^\dagger\mathbf{f})\right).
\end{aligned} \tag{4.9}$$

Note that the SM Higgs mass parameter (μ_ϕ^2) can be turned negative proportional to μ_h^2 and/or μ_k^2 in going from high energy to low energy as long as either λ_4 or λ_5 is positive. Such a choice is consistent with the boundedness conditions given in Eq. (4.4), thus enabling radiative EWSB within the model.

C. Solution to the RGEs

To find the solution to the full set of RGEs, one requires to completely specify the values of all the parameters of the Lagrangian at some energy scale. We specify the sample values at low energy scale while satisfying the necessary and sufficient conditions for the boundedness of the scalar potential in Table II.

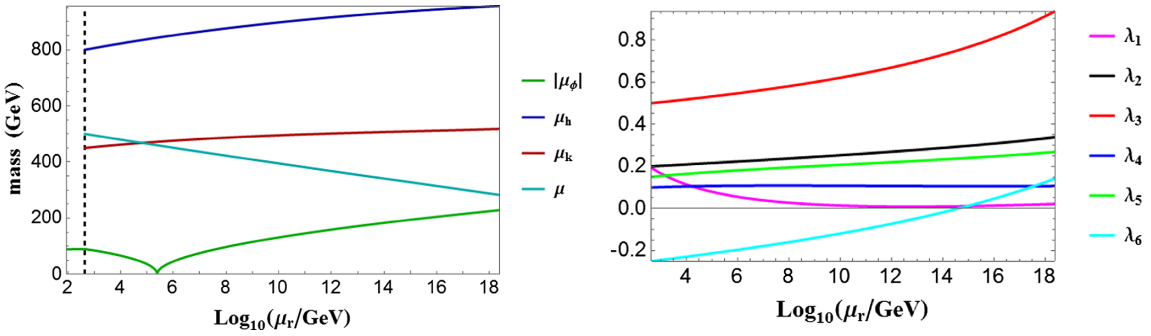

(a) Evolution of mass parameters

(b) Evolution of quartic couplings

FIG. 4. One-loop running of the parameters of two-loop neutrino mass model from the Planck scale down to the weak scale. The black dashed line corresponds to the scale $\mu_r = \mu_0$. Here μ_0 is the energy scale corresponding to the lightest of the newly introduced particles. In this sample point $\mu_o = \mu_k$. In Fig. 4(a) the evolution of the absolute value of the SM Higgs mass parameter $(|\mu_\phi|)$ along with μ_h, μ_k and cubic coupling μ has been plotted. The point at which $|\mu_\phi|$ touches the horizontal line corresponding to mass = 0 GeV is the energy scale where radiative EWSB is triggered as the sign that the SM Higgs mass-squared parameter (μ_ϕ^2) switches from positive to negative while evolving from high to low energies. Note that μ_ϕ^2 turns negative around $\mu_r \approx 10^5$ GeV, while μ_k^2 and μ_h^2 remain positive. Figure 4(b) shows the evolution of all the quartic couplings of the two-loop neutrino mass model from Planck scale down to weak scale emphasizing the fact that the model remains perturbative all the way for the selected sample point.

For the sample case, we selected the normal mass hierarchy for no specific reason. A similar result can be found if the hierarchy is inverted. We used the set of two-loop RGEs for the SM case and ran up to the lightest newly introduced scalar particle (in the sample point $\mu_0 = \mu_k$). The full set of RGEs [given in Appendix C along with Eq. (4.9)] was used to evolve the couplings and the mass parameters from the energy scale μ_0 up to the Planck scale.

In Table II only the value of $|\mathbf{f}_{\mu\tau}|$ is listed as the other values of the Yukawa couplings $\mathbf{f}$ can be calculated using Eq. (4.6) and the definitions in Eq. (4.8). For the case of the Yukawa couplings $\mathbf{h}$, we only kept the value of $|\mathbf{h}_{\mu\mu}|$ nonzero as in the fit to neutrino masses within this model, $|\mathbf{h}_{\mu\mu}| \gg |\mathbf{h}_{ij}|$ for all $i, j \neq 2, 2$ [27].

Upon performing a numerical analysis to solve the full set of RGEs for the model, we plot the evolution of all the mass parameters and the quartic couplings of the model in Fig. 4. The sample point satisfies all the necessary and sufficient boundedness conditions given in Eq. (4.4) and Fig. 4(b) ensures that all the quartic couplings stay within the perturbative range up to the Planck scale. As we have plotted the absolute value of the SM Higgs mass parameter ($|\mu_\phi|$), the point at which the plot of $|\mu_\phi|$ touches the horizontal axis (i.e. mass = 0 GeV) corresponds to the energy scale where the positive mass-squared parameter (μ_ϕ^2) turns negative at low energy, triggering radiative EWSB. For the selected sample point, the radiative correction manages to push the Higgs mass parameter in such a way that it acquires a negative value at the energy scale $\mu_r \approx 10^5$ GeV.

V. INERT DOUBLET MODEL

The inert doublet model is one of the simplest extensions of the SM, which can be treated as a special case of the more general two Higgs doublet model. In this model, the Lagrangian has a $\mathbb{Z}_2$ symmetry that remains unbroken by the vacuum structure. Even though it was introduced in the 1970s [10], it received a new influx of attention when the model was shown to be able to alleviate the issue of nondiscovery of the Higgs boson up to a mass of 115 GeV [30], address the issue of the smallness of the neutrino masses either via the type-I seesaw mechanism or via one-loop radiative mechanism (in a version referred to as the Scotogenic model) [11], leptogenesis [31] by including TeV scale right-handed neutrino, and most importantly explain dark matter of the Universe [11]. It has been shown that electroweak symmetry breaking can be induced by loop effects due to the cross coupling between the SM Higgs boson and the dark matter candidate of the model [32]. We study the scotogenic version of inert doublet model for completeness which contains a dark matter candidate and generates a naturally suppressed neutrino mass at one-loop level. Unlike the general inert doublet model, in the scotogenic version the right-handed neutrinos with sufficiently large masses can, via loop effect, turn the mass parameter of the inert doublet scalar negative in going from low to high energy, thus breaking the $\mathbb{Z}_2$ symmetry at a high scale. In this situation, the model cannot have a dark matter candidate and the neutrino masses are not naturally suppressed any more [33]. We consider TeV scale right-handed neutrino masses to avoid such an undesired situation.

A. The model

The scotogenic version of the inert doublet model requires three right-handed neutrinos (N_i) along with inert scalar doublet (η) and the SM particles. All the newly introduced particles are charged under the additional $\mathbb{Z}_2$ parity symmetry while all the SM particles are neutral under this parity. The neutral component of the inert scalar doublet is the only dark matter matter candidate for the general inert doublet model while for the scotogenic case the lightest $\mathbb{Z}_2$ odd particle—either a neutral scalar from the doublet, or the right-handed neutrino—is a dark matter candidate. The survival of the $\mathbb{Z}_2$ symmetry is crucial for the model as this symmetry protects the DM candidate from decaying and the same symmetry forbids the neutrinos from acquiring masses at tree level.

In this model, the right-handed neutrinos get a direct Majorana mass term $\frac{1}{2}\overline{N_R^i} M_{ij} N_R^{j^c} + \text{H.c.}$ which leads to masses M_i's (where $i = 1, 2, 3$) upon diagonalization. As the right-handed neutrinos are odd under the $\mathbb{Z}_2$ symmetry, the neutrino masses cannot be generated at tree level. The Lagrangian contains a neutrino Yukawa coupling involving the inert scalar doublet η and the right-handed neutrinos in addition to the SM lepton doublets. This term is given by

$$\mathcal{L}_Y \supset -\mathbf{h}_{ij}\overline{N_R^i}\tilde{\eta}^\dagger \ell_L^j + \text{H.c.}; \quad \text{where } \tilde{\eta} = i\sigma_2\eta^*. \tag{5.1}$$

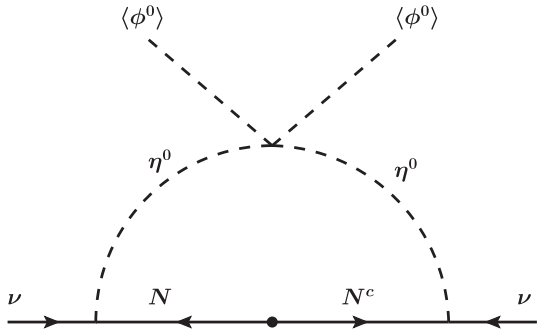

FIG. 5. Diagrammatic representation of neutrino mass generation in the scotogenic model.

This additional Yukawa coupling along with the right-handed neutrino Majorana mass term generates the loop suppressed neutrino mass matrix (see Fig. 5).

The scalar potential of the model can be written as

$$V(\phi,\eta) = \mu_\phi^2\phi^\dagger\phi + \mu_2^2\eta^\dagger\eta + \frac{\lambda_1}{2}(\phi^\dagger\phi)^2 + \frac{\lambda_2}{2}(\eta^\dagger\eta)^2 + \lambda_3(\phi^\dagger\phi)(\eta^\dagger\eta) + \lambda_4(\eta^\dagger\phi)(\phi^\dagger\eta) + \frac{\lambda_5}{2}[(\eta^\dagger\phi)^2 + \text{H.c.}]. \quad (5.2)$$

In the potential, the mass parameters $\mu_i^2 (i = 1, 2)$ and the couplings $\lambda_i, (i = 1{-}4)$ must be real. λ_5 can also be taken to be real without any loss of generality as the phase of the coupling can be absorbed by the redefinition of the η field.

B. The stability conditions and the evolution of mass parameters

The parameters in the scalar potential have to satisfy the boundedness conditions at all energy scales which ensures that the potential is bounded from below all the way. The conditions are given as

$$\lambda_1 \geq 0; \qquad \lambda_2 \geq 0; \qquad \lambda_3 \geq -\sqrt{\lambda_1\lambda_2}; \qquad \lambda_3 + \lambda_4 - |\lambda_5| \geq -\sqrt{\lambda_1\lambda_2}. \quad (5.3)$$

One can also find the physical scalar mass spectrum as

$$m_h^2 = 2\lambda_1 v^2; \quad m_\pm^2 = m_2^2 + \lambda_3 v^2; \quad m_R^2 = m_2^2 + v^2(\lambda_3 + \lambda_4 + \lambda_5); \quad m_I^2 = m_2^2 + v^2(\lambda_3 + \lambda_4 - \lambda_5), \quad (5.4)$$

where m_h is the mass of the SM Higgs boson, $m_\pm$ is the mass of the charged component of η doublet, and m_R and m_I are respectively the masses of the real and imaginary component of the neutral field inside the η doublet. We choose the real part of neutral scalar η as the DM candidate. For this scenario, the charged component of the electroweak doublet η needs to be heavier than the neutral component. Also by keeping λ_5 negative and small, we get a slightly heavier pseudo-scalar.

To illustrate the radiative electroweak symmetry breaking mechanism, we study the RGEs for the mass parameters of the scotogenic version of the inert doublet model which are given by [33]

$$16\pi^2\frac{d\mu_\phi^2}{dt} = 6\lambda_1\mu_\phi^2 + 2(2\lambda_3 + \lambda_4)\mu_2^2 + \mu_\phi^2\left[2T - \frac{3}{2}(g_1^2 + 3g_2^2)\right];$$

$$16\pi^2\frac{d\mu_2^2}{dt} = 6\lambda_2\mu_2^2 + 2(2\lambda_3 + \lambda_4)\mu_\phi^2 + \mu_2^2\left[2T_\nu - \frac{3}{2}(g_1^2 + 3g_2^2)\right] - 4\sum_{i=1}^{3} M_i^2(\mathbf{h}\mathbf{h}^\dagger)_{ii}; \quad (5.5)$$

where $T_\nu \equiv \text{Tr}[\mathbf{h}^\dagger\mathbf{h}]$.

The complete set of RGEs is given in Appendix D. The last term of the RGE for the mass parameter for scalar η, namely μ_2^2, shows its dependency on the RH neutrino mass term. For a larger value, this becomes the dominating term and pulls down the mass parameter, ultimately making it negative at higher energy. This in turns breaks the precious $\mathbb{Z}_2$ symmetry spoiling the model completely. If M_i^2 is of the same order as μ_2^2, this outcome will not be realized, and $\mathbb{Z}_2$ will remain unbroken even at higher energies.

C. Solution to the RGEs

A sample point (given in Table III) generates the running of the mass parameters and the scalar quartic couplings shown in Fig. 6. The sample point maintains all the boundedness conditions at all energy scales. The decoupling of the three RH nautrinos was only considered for the running of the mass parameter μ_2^2. As for all the other cases as the dependence on the RH neutrino mass is indirect, the decoupling effect is negligible.

In Fig. 6(a), below the energy level corresponding to the point where $\mu_\phi^2 = 0$, the electroweak symmetry is broken and the masses of the components of the scalar doublet η are split. For the energies below that point the running of the masses of the charged and neutral components of the scalar η is shown. Note that the split in the masses for the sample point is very small ($\approx$6 GeV). All the quartic couplings remain in the pertubative range and the new Yukawa couplings are chosen to be small $\mathbf{h}_{ij} \lesssim \mathcal{O}(.1)$.

TABLE III. Quartic coupling and mass parameter values for the sample point used for the inert doublet model in Fig. 6.

Quartic couplings	Values	Mass parameters	Values
$\lambda_1(m_Z)$	0.258	$\mu_2^2(\mu_2)$	800^2 (GeV)^2
$\lambda_1(\mu_2)$	0.173	M_1	900 GeV
$\lambda_2(\mu_2)$	0.35	M_2	1500 GeV
$\lambda_3(\mu_2)$	0.38	M_3	2000 GeV
$\lambda_4(\mu_2)$	−0.29	$v(m_Z)$	174.10 GeV
$\lambda_5(\mu_2)$	−0.01	μ_ϕ^2(125 GeV)	$-(88.91)^2$ (GeV)^2
		$\mu_\phi^2(\mu_2)$	$-(89.77)^2$ (GeV)^2

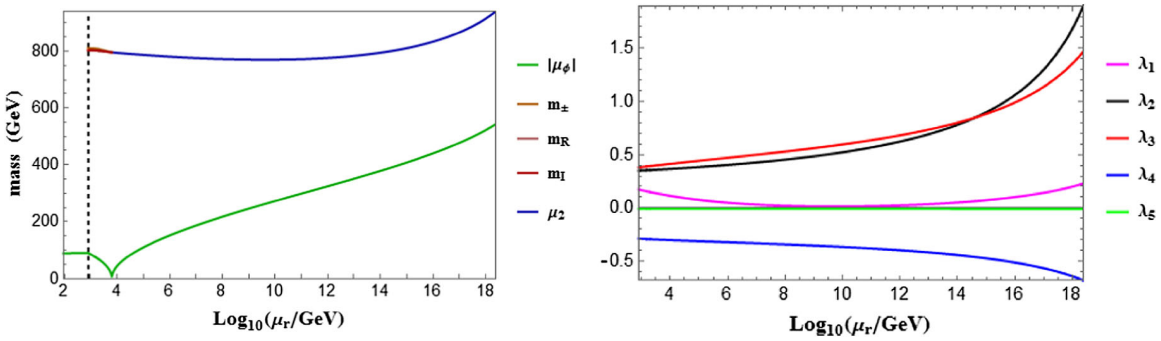

(a) Evolution of mass parameters

(b) Evolution of quartic couplings

FIG. 6. One-loop running of the parameters of scotogenic version of the inert doublet model from Planck scale down to weak scale. The black dashed line corresponds to the scale, $\mu_r = \mu_2$. In Fig. 6(a) the evolution of the absolute value of the SM Higgs mass parameter ($|\mu_\phi|$) along with the masses of the components of the inert doublet has been plotted. The point at which $|\mu_\phi|$ touches the horizontal line corresponding to mass = 0 GeV is the energy scale where radiative EWSB is triggered as the sign of the SM Higgs mass-squared parameter (μ_ϕ^2) switches from positive to negative while evolving from high to low energies. Note that μ_ϕ^2 turns negative around $\mu_r \approx 6$ TeV, while μ_2^2 remains positive all the way up to the Planck scale emphasizing the fact that the $\mathbb{Z}_2$ remains unbroken. As below $\mu_r \approx 3$ TeV, electroweak symmetry has been broken, and the common mass parameter (μ_2) for the components of inert doublet splits into $m_\pm$, m_R, and m_I. Figure 6(b) shows the evolution of all the quartic couplings of the model from the Planck scale down to weak scale. Note that the model remains perturbative all the way for the selected sample point.

VI. SCALAR SINGLET DARK MATTER MODEL

Perhaps the simplest extension of the SM requires the existence of a new heavy real scalar singlet of the SM gauge group. An unbroken $\mathbb{Z}_2$ symmetry is assumed under which the singlet scalar is odd and can serve as a candidate for dark mater [34]. Dark matter annihilation occurs efficiently in this model via Higgs portal interactions.

A. The model

In this simple extension of the SM, the added singlet can be protected from decaying into SM particles by virtue of a $\mathbb{Z}_2$ parity symmetry. This scenario can be well motivated from some higher symmetry at the GUT scale where all the other additional particles lie above some intermediate scale. For example, such a stable dark matter can be easily incorporated in $SO(10)$ models [35]. In such cases, the low scale scalar potential becomes

$$V(\phi, s) = \mu_\phi^2 \phi^\dagger \phi + \frac{\mu_s^2}{2} s^2 + \frac{\lambda_1}{2} (\phi^\dagger \phi)^2 + \frac{\lambda_2}{8} s^4 + \frac{\lambda_3}{2} (\phi^\dagger \phi) s^2. \tag{6.1}$$

Below the energy scale corresponding to the mass of the singlet, the effective quartic coupling is given by

$$\lambda_1^{\text{eff}} = \lambda_1 - \frac{\lambda_3^2}{\lambda_2}. \tag{6.2}$$

And the mass of the observed Higgs particle is $m_h^2 = 2\lambda_1^{\text{eff}} v^2$ and the matching condition Eq. (6.2) is needed while one evolves the RGE for the Higgs quartic coupling.

B. The stability conditions and the evolution of the mass parameters

The parameters of the scalar potential must obey the boundedness constraints so that the potential remains bounded from below. The conditions for this simple potential are given as

$$\lambda_1 \geq 0; \qquad \lambda_2 \geq 0; \qquad \lambda_3 \geq -\sqrt{\lambda_1 \lambda_2}. \tag{6.3}$$

For this extension of the SM, most of the RGEs of the SM remain the same. But one should update the RGEs for the Higgs quartic coupling (λ_1) and the Higgs mass parameters (μ_ϕ^2) along with the newly introduced quartic couplings (λ_2, λ_3) and mass parameter (μ_s^2). The full set of new and updated RGEs is given in Appendix E. The RGEs of the mass parameters are given as

$$16\pi^2 \frac{d\mu_\phi^2}{dt} = \left[6\lambda_1 + 2T - \frac{9}{10} g_1^2 - \frac{9}{2} g_2^2\right] \mu_\phi^2 + \lambda_3 \mu_s^2;$$
$$16\pi^2 \frac{d\mu_s^2}{dt} = 3\lambda_2 \mu_s^2 + 4\lambda_3 \mu_\phi^2. \tag{6.4}$$

From the RGEs of the mass parameters, one immediately notices that the coupling λ_3 has the potential to turn the mass parameter of the SM Higgs negative at low energy while it remains positive at high energy. And one also notices that one needs a lower bound on coupling λ_3 to perform such a mechanism. The quartic coupling λ_3 is also the coupling that keeps the dark matter in thermal equilibrium. So a lower limit needed for the radiative electroweak symmetry breaking can be translated into a lower

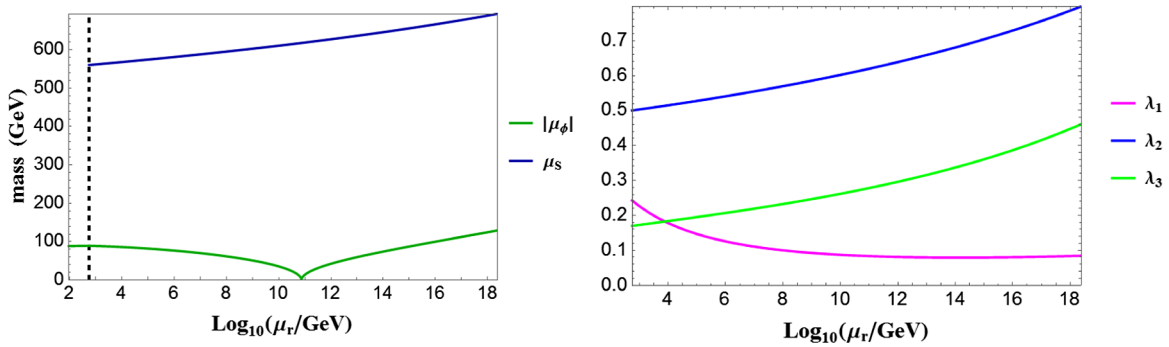

(a) Evolution of mass parameters

(b) Evolution of quartic couplings

FIG. 7. One-loop running of the parameters of the scalar singlet dark matter model from the Planck scale down to the weak scale. The black dashed line corresponds to the scale $\mu_r = \mu_s$. In (a) the evolution of the absolute value of the SM Higgs mass parameter ($|\mu_\phi|$) along with the mass of the dark matter candidate has been plotted. The point at which $|\mu_\phi|$ touches the horizontal line corresponding to mass $= 0$ GeV is the energy scale where radiative EWSB is triggered as the sign of the SM Higgs mass-squared parameter (μ_ϕ^2) switches from positive to negative while evolving from high to low energies. Note that μ_ϕ^2 turns negative around $\mu_r \approx 10^{11}$ GeV, while μ_s^2 remains positive all the way up to the Planck scale emphasizing the fact that the $\mathbb{Z}_2$ that protects the dark matter candidate remains unbroken. (b) shows the evolution of all the quartic couplings of the model from the Planck scale down to the weak scale. Note that the model remains perturbative all the way for the selected sample point.

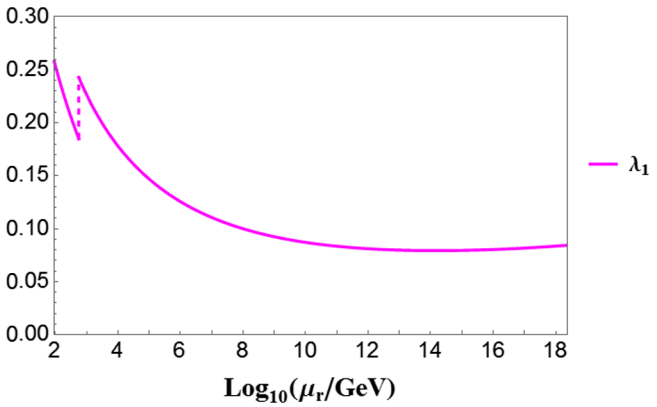

FIG. 8. Running of the SM Higgs quatic coupling in the extension of the SM by a real scalar singlet. The discontinuous shift in the plot at the renormalization energy scale ≈560 GeV corresponds to the affect of the real scalar singlet. Below that energy scale, the effective Higgs quartic coupling given by Eq. (6.2) has been considered.

limit on the dark matter mass if one assumes that the thermal relic abundance of the dark matter is in agreement with the observed density, $\Omega_{\rm DM}h^2 \simeq 0.1186$. Here $\Omega_{\rm DM}$ is the critical mass density for dark matter and h is the Hubble constant in units of 100 km.(s. Mpc). The mass of the dark matter candidate is given by $m_s^2 = m_{\rm DM}^2 = \frac{\lambda_3}{2}v^2 + \mu_s^2$ and also assuming standard thermal freeze-out, we get $m_{\rm DM} \simeq 3.3\lambda_3$ TeV.

Furthermore, according to Eq. (E1) the contribution of the quartic couplings λ_3 to the SM Higgs quartic coupling is just perfect to make the electroweak vacuum stable all the way to the Planck scale.

C. Solution to the RGEs

Like the previous cases, we evolved the SM couplings and parameters at two-loop level up to the energy scale corresponding to the mass of the singlet. From that point we evolved the new set of RGEs at one loop level up to the Planck scale.

We randomly took a sample point (given in Table IV) to illustrate the radiative electroweak symmetry breaking scenario for this extension of the SM. The running in Fig. 7(a) is from the mass of the singlet to the Planck scale, while Fig. 7(b) is from the weak scale to the Planck scale. To show the evolution of the SM Higgs quartic coupling we evolved the $\lambda_1^{\rm eff}$ up to the singlet mass using two-loop SM RGEs and then used the matching condition in Eq. (6.2) and the set of updated RGEs to run the coupling up to the Planck scale (see Fig. 8). This figure also shows that the electroweak vacuum is perfectly stable for the selected sample point.

VII. UNIVERSAL SEESAW MODEL WITH VECTORLIKE FERMIONS

In universal seesaw models, one introduces a new set of heavy vectorlike fermions which are responsible for the masses for quarks and charged leptons via a generalized seesaw mechanism [36]. Besides providing an explanation of the smallness of the masses of fermions like u, d, e, etc. in the context of left-right symmetry, a CP phenomenology study has revealed that such a model also harbors a solution for the strong CP problem as the $\bar{\theta}$ parameter of the strong CP problem only has nonzero value ($\bar{\theta} \sim 10^{-12}$) at the two-loop level [36–39]. Here we propose and analyze a $SM \times U(1)$ based universal seesaw model without commenting on left-right symmetry. The strong CP problem

TABLE IV. Quartic coupling and mass parameter values for the sample point used for the extension of the SM by a real scalar singlet in Fig. 7. Note that the mass parameter of the dark matter candidate μ_s^2 corresponds to the value needed for the right amount of thermal relic abundance.

Quartic couplings	Values	Mass parameters	Values
$\lambda_1^{\rm eff}(m_Z)$	0.258	μ_s^2	560^2 (GeV)^2
$\lambda_1^{\rm eff}(\mu_s)$	0.1887	$v(m_Z)$	174.10 GeV
$\lambda_1(\mu_s)$	0.247	μ_ϕ^2(125 GeV)	$-(88.91)^2$ (GeV)^2
$\lambda_2(m_s)$	0.5	$\mu_\phi^2(\mu_s)$	$-(89.63)^2$ (GeV)^2
$\lambda_3(m_s)$	0.17		

may be solved via spontaneous CP violation [40]. The presence of new scalars needed for $U(1)$ symmetry breaking enables us to realize radiative EWSB.

A. The model

The model under scrutiny uses the seesaw mechanism for quarks and leptons and is based upon the assumption that there exists a set of TeV scale vectorlike fermions. The original version of the model was constructed in the context of a left-right symmetric model [36]. Here we will study a variant of the model which is based on an extension of the SM gauge sector by an $U(1)_X$, where all the left-handed fermions of the SM are neutral under the new gauge group while the TeV scale vectorlike fermions are not. The model requires two more additional scalar bosons (S_1 and S_2) along with the SM Higgs doublet with the quantum charge assignment for all the particles of the model is listed in the Table V. While one singlet scalar S_1 or S_2 is sufficient for $U(1)$ symmetry breaking, both scalars are needed for seesaw mass generation.

The vev of the singlet S_2 gives masses to the vectorlike fermions and the vev of S_1 along with the electroweak vev mixes the right- and left-handed quarks (and leptons) with the vectorlike quarks (and leptons) while the $U(1)_X$ symmetry forbids the bare mass terms of any of the vectorlike fermions. Thus, this model is a natural framework for the universal seesaw mechanism related without left-right symmetry.

TABLE V. Particle content of the vectorlike fermion model.

Particle	$(SU(3)_C \times SU(2)_L \times U(1)_Y \times U(1)_X)$
$\mathcal{Q}$	$(3,2,\frac{1}{6},0)$
$\mathcal{L}$	$(1,2,-\frac{1}{2},0)$
u^c	$(\bar{3},1,-\frac{2}{3},-2)$
d^c	$(\bar{3},1,\frac{1}{3},2)$
e^c	$(1,1,-1,2)$
U	$(3,1,\frac{2}{3},1)$
U^c	$(\bar{3},1,-\frac{2}{3},1)$
D	$(3,1,-\frac{1}{3},-1)$
D^c	$(\bar{3},1,\frac{1}{3},-1)$
E	$(1,1,1,-1)$
E^c	$(1,1,-1,-1)$
ϕ	$(1,2,\frac{1}{2},-1)$
S_1	(1,1,0,1)
S_2	$(1,1,0,-2)$

Note that the setup is anomaly free. As the added fermions are vectorlike, most of the anomalies cancel trivially. The only nontrivial cancellations are for the cases $U(1)_Y[U(1)_X]^2$, $[U(1)_Y]^2U(1)_X$, and $\mathrm{Tr}[U(1)_X]$. A straightforward calculation using Table V shows that the anomalies for these three cases are all zero.

The Yukawa sector of the Lagrangian for this model is given by

$$\begin{aligned}\mathcal{L}_Y = {} & \mathbf{Y_u}\mathcal{Q}U^c\phi + \mathbf{F_u}Uu^cS_1 + \mathbf{G_u}UU^cS_2 \\ & - \mathbf{Y_d}\mathcal{Q}D^c\tilde{\phi} + \mathbf{F_d}Dd^cS_1^* + \mathbf{G_d}DD^cS_2^* \\ & - \mathbf{Y_e}\mathcal{L}E^c\tilde{\phi} + \mathbf{F_e}Ee^cS_1^* + \mathbf{G_e}EE^cS_2^* + \mathrm{H.c.} \end{aligned} \tag{7.1}$$

where

$$\begin{aligned}\mathbf{Y_u}\mathcal{Q}U^c\phi &= (\mathbf{Y_u})_{ij}(u_iU_j^c\phi^0 - d_iU_j^c\phi_u^+); \\ -\mathbf{Y_d}\mathcal{Q}D^c\tilde{\phi} &= (\mathbf{Y_d})_{ij}(u_iD_j^c\phi^- + d_iD_j^c\bar{\phi}^0); \\ -\mathbf{Y_e}\mathcal{L}E^c\tilde{\phi} &= (\mathbf{Y_e})_{ij}(\nu_iE_j^c\phi^- + e_iE_j^c\bar{\phi}^0); \end{aligned} \tag{7.2}$$

and

$$\phi = \begin{pmatrix}\phi^+ \\ \phi^0\end{pmatrix}; \qquad \tilde{\phi} = \begin{pmatrix}\bar{\phi}^0 \\ \phi^-\end{pmatrix} \tag{7.3}$$

When the electroweak doublet and scalar singlets both get vevs, one acquires the fermion mass matrix $\mathcal{M}_f$ in the seesaw form for both quark and lepton as

$$\mathcal{M}_f = \begin{pmatrix}0 & \frac{1}{\sqrt{2}}\mathbf{Y_f}v \\ \mathbf{F_f}v_{s_1} & \mathbf{G_f}v_{s_2}\end{pmatrix} \tag{7.4}$$

where $\mathbf{f} = \mathbf{u}, \mathbf{d}, \mathbf{e}$. For such a case the mass of the light quark (or lepton) becomes $m_f \approx \frac{Y_fF_fvv_{s_1}}{\sqrt{2}G_fv_{s_2}}$. Since these masses scale quadratically with Yukawa couplings, fermion mass hierarchy may be explained with only a mild hierarchy $\sim(10^{-2}$–$10^{-3})$ in the Yukawa couplings.

The scalar potential of the model can be written as

$$\begin{aligned}V(\phi,S_1,S_2) = {} & \mu_\phi^2\phi^\dagger\phi + \mu_1^2S_1^*S_1 + \mu_2^2S_2^*S_2 \\ & - (\mu S_1^2S_2 + \mathrm{H.c.}) + \frac{\lambda_1}{2}(\phi^\dagger\phi)^2 + \frac{\lambda_2}{2}(S_1^*S_1)^2 \\ & + \frac{\lambda_3}{2}(S_2^*S_2)^2 + \lambda_4(\phi^\dagger\phi)(S_1^*S_1) \\ & + \lambda_5(\phi^\dagger\phi)(S_2^*S_2) + \lambda_6(S_1^*S_1)(S_2^*S_2). \end{aligned} \tag{7.5}$$

Here μ can be taken as real without any loss of generality by the redefinition of the complex scalar S_2.

When the scalar S_1 develops a vev v_{s_1} via radiative corrections (see below), the S_2 develops an induced vev due to the linear term in S_2 in the potential. For such a case, the imaginary part of the complex scalar S_1 is absorbed by the broken generator of $U(1)_X$ and the mass matrix for the scalar becomes

$$\mathcal{M}_s^2 = \begin{pmatrix} 2\lambda_1 v^2 & 2\lambda_4 v v_{s_1} & 0 & 0 \\ 2\lambda_4 v v_{s_1} & 2\lambda_2 v_{s_1}^2 & -2\mu v_{s_1} & 0 \\ 0 & -2\mu v_{s_1} & \lambda_5 v^2 + \lambda_6 v_{s_1}^2 + \mu_2^2 & 0 \\ 0 & 0 & 0 & \lambda_5 v^2 + \lambda_6 v_{s_1}^2 + \mu_2^2 \end{pmatrix}. \tag{7.6}$$

Here the basis of the matrix $\mathcal{M}_s^2$ is $\{m_h, m_{S_1}, m_{S_{2R}}, m_{S_{2I}}\}$, where m_h is the SM Higgs, and m_{S_1} is the mass of the singlet S_1 and the $m_{S_{2R}}, m_{S_{2I}}$ are the masses of the real and imaginary part of the S_2 scalar. From the potential we find that the induced vev for the scalar S_2 is given by

$$v_{s_2} = \frac{\sqrt{2}\mu v_{s1}^2}{\lambda_5 v^2 + \lambda_6 v_{s_1}^2 + \mu_2^2}. \tag{7.7}$$

A small value of the coupling λ_4 and v_{s_1} around the TeV scale will ensure a small mixing between the SM Higgs and the singlet S_1 while the mixing between S_1 and S_2 depends on the cubic coupling parameter μ.

B. The stability condition and the evolution of the mass parameters

From the stability point of view, the scalar potential of the vectorlike fermion model and the two-loop neutrino mass model are identical. So, the stability condition given by Eq. (4.4) is applicable here too.

The RGEs for the mass parameters are found to be

$$\begin{aligned} 16\pi^2 \frac{d\mu_\phi^2}{dt} &= \mu_\phi^2 \left[6\lambda_1 - \frac{9}{10} g_1^2 - \frac{9}{2} g_2^2 - 6 g_4^2 + 2T \right] \\ &\quad + 2\lambda_4 \mu_1^2 + 2\lambda_5 \mu_2^2; \\ 16\pi^2 \frac{d\mu_1^2}{dt} &= \mu_1^2 [4\lambda_2 - 6 g_4^2 + 2T_F] + 4\lambda_4 \mu_\phi^2 + 2\lambda_6 \mu_2^2 + 8\mu^2; \\ 16\pi^2 \frac{d\mu_2^2}{dt} &= \mu_2^2 [4\lambda_3 - 24 g_4^2 + 2T_G] + 4\lambda_5 \mu_\phi^2 + 4\lambda_6 \mu_1^2 + 4\mu^2; \\ 16\pi^2 \frac{d\mu}{dt} &= \mu [2\lambda_2 + 2\lambda_6 - 18 g_4^2 + 2T_F + T_G]. \end{aligned} \tag{7.8}$$

The complete set of RGEs are given in Appendix F.

C. Solution to the RGEs

To find the solution of the set of RGEs, we took a more simplified case where we kept all the Yukawa coupling $\mathbf{F}$ to be small and negligible and Yukawa coupling $\mathbf{G} \simeq \mathcal{O}(1)$. The numerical solution was hunted for the case where one of the eigenvalues of the scalar mass matrix $\mathcal{M}_s$ corresponds to the SM Higgs boson and another one corresponds to the scalar boson of mass $\sim\mu_s$. Here, we used $\mu_s = 750$ GeV just as an example as a similar universal seesaw model [39] was used to explain apparent diphoton excess [41] which eventually became statistically insignificant [42]. The vectorlike fermion mass was kept around the TeV scale where the mass is approximated by $\sim \mathbf{G} v_{s_2}$. One such sample point is given by Table VI. As the first new particle in this model is at $\mu_s = 750$ GeV, the SM RGEs were evolved at the two-loop level up to the scale μ_s and then the new set of RGEs was deployed due to the evolution of the couplings and mass parameters. Figure 9 shows that both the vevs (electroweak vev and vev for the single S_1) can be generated by radiative correction.

TABLE VI. Quartic couplings and mass parameter values for the sample point used for the vectorlike fermion model in Fig. 9.

Quartic couplings	Values	Mass parameters	Values
$\lambda_1(m_Z)$	0.258	$\mu_1^2(\mu_s)$	$-(1800)^2$ (GeV)^2
$\lambda_1(\mu_s)$	0.175	$\mu_2^2(\mu_s)$	$(2550)^2$ (GeV)^2
$\lambda_2(\mu_s)$	0.25	$\mu_\phi^2(\mu_s)$	$-(89.74)^2$ (GeV)^2
$\lambda_3(\mu_s)$	0.24	$\mu(\mu_s)$	850 GeV
$\lambda_4(\mu_s)$	0.02	$\mu_\phi^2(125$ GeV$)$	$-(88.91)^2$ (GeV)^2
$\lambda_5(\mu_s)$	0.1	$(G_u)_{ii}(M_z) \sim (G_d)_{ii}(M_z) \sim (G_e)_{ii}(M_z)$	0.45
$\lambda_6(\mu_s)$	0.09	v_{s_1}	3.60 TeV
μ_s	750 GeV	v_{s_2}	2.26 TeV

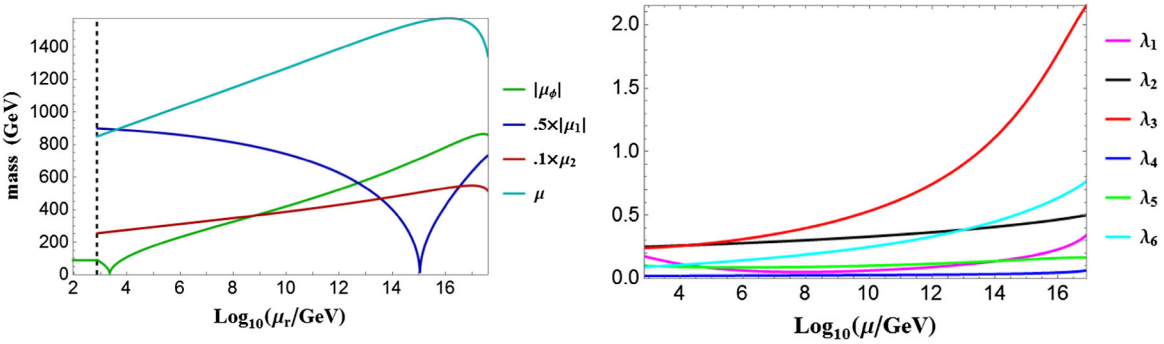

(a) Evolution of mass parameters

(b) Evolution of quartic couplings

FIG. 9. One-loop running of the couplings and mass parameters of the vectorlike fermion model. The black dashed line corresponds to the scale $\mu_r = \mu_s$. In (a) the evolution of the absolute value of the SM Higgs mass parameter ($|\mu_\phi|$) and $|\mu_1|$ along with the mass parameters μ_2 and μ have been plotted. The point at which $|\mu_\phi|$ touches the horizontal line corresponding to mass = 0 GeV is the energy scale where radiative EWSB is triggered as the sign of the SM Higgs mass-squared parameter (μ_1^2) switches from positive to negative while evolving from high to low energies. For the sample point, this happens around TeV energy scale. Note that the mass parameter of the scalar S_1 also turns negative around the renormalization energy scale $\approx 10^{15}$ GeV indicating that the $U(1)_X$ symmetry also gets broken radiatively. (b) shows the evolution of all the quartic couplings of the model from the Planck scale down to the weak scale. Note that the model remains perturbative all the way for the selected sample point.

VIII. CONCLUSION

We have presented in this paper various extensions of the SM where electroweak symmetry breaking is triggered by the renormalization group flow. Even though such symmetry breaking fails to occur in the SM, the scalar extensions are able to incorporate this attractive mechanism. Extensions like type-II seesaw models, loop-induced neutrino mass models, and scalar dark matter models all have this built-in feature. A common shared feature of all models where radiative EWSB is realized is the presence of new scalars at the TeV scale. These TeV scale scalars may be detected in the Large Hadron Collider in the near future.

ACKNOWLEDGMENTS

K. S. B. would like to thank the Bartol Research Institute for hospitality during a visit where the work was initiated. K. S. B. and S. K. would like to thank the organizers of CETUP* 2016 for hospitality and the participants for helpful discussions and comments. The work of K. S. B. and S. K. is supported in part by the U.S. Department of Energy Grant No. de-sc0016013 and the work of I. G. is supported in part by the Bartol Research Institute.

APPENDIX A: BOUNDEDNESS CONDITION FOR TYPE-II SEESAW

The gauge transformation of the fields defined in Eqs. (3.2)–(3.3) can be written as

$$\ell \to \mathcal{U}\ell; \qquad \Delta \to \mathcal{U}\Delta\mathcal{U}^\dagger \tag{A1}$$

where $\mathcal{U}$ is a unitary matrix. Under this gauge transformation the Yukawa term remains invariant:

$$\mathcal{L}_Y \supset \ell^T i\sigma_2 \Delta \ell \to \ell^T \mathcal{U}^T i\sigma_2 \mathcal{U}\Delta\mathcal{U}^\dagger\mathcal{U}\ell = \ell^T i\sigma_2\Delta\ell. \tag{A2}$$

Let us define $\hat{\Delta} = i\sigma_2\Delta$:

$$\hat{\Delta} = \begin{pmatrix} \Delta^0 & -\frac{\Delta^+}{\sqrt{2}} \\ -\frac{\Delta^+}{\sqrt{2}} & -\Delta^{++} \end{pmatrix}. \tag{A3}$$

The gauge transformation of the field $\hat{\Delta}$ can be written as

$$\hat{\Delta} \to i\sigma_2\mathcal{U}\Delta\mathcal{U}^\dagger = \mathcal{U}^*\hat{\Delta}\mathcal{U}^\dagger. \tag{A4}$$

Now, one can diagonalize $\hat{\Delta}$ by gauge transformation and as $\mathrm{Tr}(\mathcal{U}^*\hat{\Delta}\mathcal{U}^\dagger) \neq 0$, we can write $\hat{\Delta}$ in such a basis as

$$\hat{\Delta} = \begin{pmatrix} a & 0 \\ 0 & be^{i\alpha} \end{pmatrix}; \quad \text{where } a, b \text{ and } \alpha \text{ are real.} \tag{A5}$$

Let us define the Higgs doublet as

$$\phi = \begin{pmatrix} ce^{i\delta} \\ de^{i\gamma} \end{pmatrix}; \quad \text{where } c, d, \delta \text{ and } \gamma \text{ are real.} \tag{A6}$$

In terms of these real fields the quartic part of the scalar potential [given in Eq. (3.2)] becomes

$$V^{(4)} = \frac{\lambda_1}{2}u^4 + \frac{\lambda_2}{2}(a^2+b^2)^2 + \lambda_3 a^2b^2 + \lambda_4 u^2(a^2+b^2) + \lambda_5(a^2-b^2)\cos 2\beta \tag{A7}$$

where

$$c = u\cos\beta; \qquad d = u\sin\beta. \tag{A8}$$

The quartic couplings of the potential form a vector space spanned by the real valued vector, $\boldsymbol{x}^T = (u^2, a^2, b^2)$ and the quartic couplings of the scalar potential can be written as

$$V = \frac{1}{2}\boldsymbol{x}^T\boldsymbol{\lambda}\boldsymbol{x}, \tag{A9}$$

where

$$\boldsymbol{\lambda} = \begin{pmatrix} \lambda_1 & \lambda_4 + \lambda_5\cos 2\beta & \lambda_4 - \lambda_5\cos 2\beta \\ \lambda_4 + \lambda_5\cos 2\beta & \lambda_2 & \lambda_2 + \lambda_3 \\ \lambda_4 - \lambda_5\cos 2\beta & \lambda_2 + \lambda_3 & \lambda_2 \end{pmatrix}. \tag{A10}$$

We use known results from the copositivity conditions of real symmetric matrices [43,44] to determine the boundedness conditions as

$$\text{(i)} \quad \lambda_1 \geq 0; \qquad \lambda_2 \geq 0; \tag{A11}$$

$$\begin{aligned} \text{(ii)} \quad & \lambda_4 + \lambda_5\cos 2\beta \geq -\sqrt{\lambda_1\lambda_2}; \\ & \lambda_4 - \lambda_5\cos 2\beta \geq -\sqrt{\lambda_1\lambda_2}; \\ & \lambda_2 + \lambda_3 \geq -\lambda_2; \end{aligned} \tag{A12}$$

$$\text{(iii)} \quad 2\lambda_4\sqrt{\lambda_2} + 2\lambda_2\sqrt{\lambda_1} + \lambda_3\sqrt{\lambda_1} \geq 0 \quad \text{or} \quad \det\boldsymbol{\lambda} \geq 0; \tag{A13}$$

where

$$\det\boldsymbol{\lambda} = -2\lambda_1\lambda_2\lambda_3 - \lambda_1\lambda_3^2 + 2\lambda_3\lambda_4^2 - 2(2\lambda_2 + \lambda_3)\lambda_5^2\cos^2 2\beta. \tag{A14}$$

As this set of boundedness conditions need to be satisfied for all values of β, this set of conditions reduces to the set of inequalities (3.6), (3.7), and (3.8). Note that all the conditions mentioned in inequalities (3.6) and (3.7) and at least one of the conditions in inequality (3.8) need to be satisfied for the potential to be bounded from below.

APPENDIX B: COMPLETE SET OF RGES FOR TYPE-II NEUTRINO MASS MODEL

The RGEs for the Yukawa couplings are given by [24]

$$\begin{aligned}
16\pi^2\frac{d\mathbf{Y}_d}{dt} &= \mathbf{Y_d}\left[\frac{3}{2}\mathbf{Y_d^\dagger Y_d} - \frac{3}{2}\mathbf{Y_u^\dagger Y_u}\right] + \mathbf{Y_d}\left[T - \frac{1}{4}g_1^2 - \frac{9}{4}g_2^2 - 8g_3^2\right]; \\
16\pi^2\frac{d\mathbf{Y}_u}{dt} &= \mathbf{Y_u}\left[\frac{3}{2}\mathbf{Y_u^\dagger Y_u} - \frac{3}{2}\mathbf{Y_d^\dagger Y_d}\right] + \mathbf{Y_u}\left[T - \frac{17}{20}g_1^2 - \frac{9}{4}g_2^2 - 8g_3^2\right]; \\
16\pi^2\frac{d\mathbf{Y}_e}{dt} &= \mathbf{Y_e}\left[\frac{3}{2}\mathbf{Y_e^\dagger Y_e} + \frac{3}{2}\mathbf{Y_\Delta^\dagger Y_\Delta}\right] + \mathbf{Y_e}\left[T - \frac{9}{4}g_1^2 - \frac{9}{4}g_2^2\right]; \\
16\pi^2\frac{d\mathbf{Y}_\Delta}{dt} &= \left[\frac{1}{2}\mathbf{Y_e^\dagger Y_e} + \frac{3}{2}\mathbf{Y_\Delta^\dagger Y_\Delta}\right]^T\mathbf{Y}_\Delta + \mathbf{Y}_\Delta\left[\frac{1}{2}\mathbf{Y_e^\dagger Y_e} + \frac{3}{2}\mathbf{Y_\Delta^\dagger Y_\Delta}\right] + \left[-\frac{3}{2}\left(\frac{3}{5}g_1^2 + 3g_2^2\right) + \mathrm{Tr}(\mathbf{Y_\Delta^\dagger Y_\Delta})\right]\mathbf{Y}_\Delta.
\end{aligned} \tag{B1}$$

The RGEs for the quartic couplings of the Lagrangians are given by [24]

$$\begin{aligned}
16\pi^2\frac{d\lambda_1}{dt} &= 12\lambda_1^2 - 3\lambda_1\left(3g_2^2 + \frac{3}{5}g_1^2\right) + 3g_2^4 + \frac{3}{2}\left(\frac{3}{5}g_1^2 + g_2^2\right)^2 + 4\lambda_1 T - 8H + 12\lambda_4^2 + 8\lambda_5^2; \\
16\pi^2\frac{d\lambda_2}{dt} &= -\frac{36}{5}g_1^2\lambda_2 - 24g_2^2\lambda_2 + \frac{108}{25}g_1^4 + 18g_2^4 + \frac{72}{5}g_1^2g_2^2 + 14\lambda_2^2 + 4\lambda_2\lambda_3 + 2\lambda_3^2 + 4\lambda_4^2 + 4\lambda_5^2 \\
&\quad + 4\mathrm{Tr}(\mathbf{Y_\Delta^\dagger Y_\Delta})\lambda_2 - 8\mathrm{Tr}(\mathbf{Y_\Delta^\dagger Y_\Delta Y_\Delta^\dagger Y_\Delta}); \\
16\pi^2\frac{d\lambda_3}{dt} &= -\frac{36}{5}g_1^2\lambda_3 - 24g_2^2\lambda_3 + 12g_2^4 - \frac{144}{5}g_1^2g_2^2 + 3\lambda_3^2 + 12\lambda_2\lambda_3 - 8\lambda_5^2 + 4\mathrm{Tr}(\mathbf{Y_\Delta^\dagger Y_\Delta})\lambda_3 + 8\mathrm{Tr}(\mathbf{Y_\Delta^\dagger Y_\Delta Y_\Delta^\dagger Y_\Delta}); \\
16\pi^2\frac{d\lambda_4}{dt} &= -\frac{9}{2}g_1^2\lambda_4 - \frac{33}{2}g_2^2\lambda_4 + \frac{27}{25}g_1^4 + 6g_2^4 + [8\lambda_2 + 2\lambda_3 + 6\lambda_1 + 4\lambda_4 + 2T + 2\mathrm{Tr}(\mathbf{Y_\Delta^\dagger Y_\Delta})]\lambda_4 + 8\lambda_5^2; \\
16\pi^2\frac{d\lambda_5}{dt} &= -\frac{9}{2}g_1^2\lambda_5 - \frac{33}{2}g_2^2\lambda_5 - \frac{18}{5}g_1^2g_2^2 + [2\lambda_2 - 2\lambda_3 + 2\lambda_1 + 8\lambda_4 + 2T + 2\mathrm{Tr}(\mathbf{Y_\Delta^\dagger Y_\Delta})]\lambda_5, \\
\text{where } T &= \mathrm{Tr}[\mathbf{Y_e^\dagger Y_e} + 3\mathbf{Y_d^\dagger Y_d} + 3\mathbf{Y_u^\dagger Y_u}]; \quad H = \mathrm{Tr}[\mathbf{Y_e^\dagger Y_e Y_e^\dagger Y_e} + 3\mathbf{Y_d^\dagger Y_d Y_d^\dagger Y_d} + 3\mathbf{Y_u^\dagger Y_u Y_u^\dagger Y_u}].
\end{aligned} \tag{B2}$$

The RGEs for the mass parameters are given by Eq. (3.10).

Beyond the energy scale corresponding to the mass of the triplet (μ_Δ), the SM gauge coupling evolution also needs to be recalculated due to the triplet's contribution. While the weak triplet does not affect the evolution of the $SU(3)_C$ gauge coupling evolution, it does change the RGEs of the other gauge couplings. The RGEs for the gauge couplings are given by

$$16\pi^2 \frac{dg_i}{dt} = b_i g_i^3, \tag{B3}$$

where $g_i = \{g_3, g_2, g_1\}$ are the three gauge couplings with the one-loop β-function coefficient $b_i = \{-7, -\frac{5}{2}, \frac{47}{10}\}$.

APPENDIX C: COMPLETE SET OF RGES FOR TWO-LOOP NEUTRINO MASS MODEL

For the two-loop neutrino mass model, among the gauge couplings only the hypercharge gauge coupling is modified due the additional scalar particles. So, the RGEs for the SM gauge couplings are given by

$$16\pi^2 \frac{dg_i}{dt} = b_i g_i^3, \tag{C1}$$

where $g_i = \{g_3, g_2, g_1\}$ are the three gauge couplings with the one-loop β-function coefficient $b_i = \{-7, -\frac{19}{6}, \frac{51}{10}\}$.

The RGEs for the Yukawa couplings are given by [27]

$$\begin{aligned}
16\pi^2 \frac{d\mathbf{h}}{dt} &= 4(\mathbf{h}\mathbf{h}^\dagger\mathbf{h}) + 4\mathbf{h}\mathrm{Tr}(\mathbf{h}^\dagger\mathbf{h}) - \frac{18}{5} g_1^2 \mathbf{h} + \frac{1}{2}(h\mathbf{Y}_\ell^\dagger \mathbf{Y}_\ell) \\
&\quad + \frac{1}{2}(\mathbf{Y}_\ell^T \mathbf{Y}_\ell^* h); \\
16\pi^2 \frac{d\mathbf{f}}{dt} &= 4(\mathbf{f}\mathbf{f}^\dagger\mathbf{f}) + 4\mathbf{f}\mathrm{Tr}(\mathbf{f}^\dagger\mathbf{f}) + \frac{1}{2}(\mathbf{f}\mathbf{Y}_\ell \mathbf{Y}_\ell^\dagger) + \frac{1}{2}(\mathbf{Y}_\ell^* \mathbf{Y}_\ell^{\mathbf{T}} \mathbf{f}) \\
&\quad - \frac{3}{2}\mathbf{f}\left(-\frac{3}{5} g_1^2 + g_2^2\right).
\end{aligned} \tag{C2}$$

The RGEs for the quartic scalar couplings are given by [27,45]

$$\begin{aligned}
16\pi^2 \frac{d\lambda_1}{dt} &= 12\lambda_1^2 + 2\lambda_4^2 + 2\lambda_5^2 - \lambda_1\left(9g_2^2 + \frac{9}{5} g_1^2\right) + \frac{9}{4} g_2^4 + \frac{27}{100} g_1^4 + \frac{9}{10} g_2^2 g_1^2 + 4\lambda_1 T - 4H; \\
16\pi^2 \frac{d\lambda_2}{dt} &= 10\lambda_2^2 + 4\lambda_4^2 + 2\lambda_6^2 - \frac{36}{5}\lambda_2 g_1^2 + \frac{108}{25} g_1^4 + 16\lambda_2 \mathrm{Tr}(\mathbf{f}^\dagger\mathbf{f}) - 32\mathrm{Tr}(\mathbf{f}^\dagger\mathbf{f})^2; \\
16\pi^2 \frac{d\lambda_3}{dt} &= 10\lambda_3^2 + 4\lambda_5^2 + 2\lambda_6^2 - \frac{144}{5}\lambda_2 g_1^2 + \frac{864}{25} g_1^4 + 16\lambda_3 \mathrm{Tr}(\mathbf{h}^\dagger\mathbf{h}) - 64\mathrm{Tr}(\mathbf{h}^\dagger\mathbf{h})^2; \\
16\pi^2 \frac{d\lambda_4}{dt} &= 6\lambda_1\lambda_4 + 4\lambda_2\lambda_4 + 2\lambda_5\lambda_6 + 4\lambda_4^2 - \lambda_4\left(\frac{9}{2} g_2^2 + \frac{45}{10} g_1^2\right) + \frac{27}{50} g_1^4 + 2\lambda_4[4\mathrm{Tr}(\mathbf{f}^\dagger\mathbf{f}) + T] - 8\mathrm{Tr}(\mathbf{f}^\dagger\mathbf{f}\mathbf{Y}_\ell^\dagger\mathbf{Y}_\ell);
\end{aligned} \tag{C3}$$

$$\begin{aligned}
16\pi^2 \frac{d\lambda_5}{dt} &= 6\lambda_1\lambda_5 + 4\lambda_3\lambda_5 + 2\lambda_4\lambda_6 + 4\lambda_5^2 - \lambda_5\left(\frac{9}{2} g_2^2 + \frac{153}{10} g_1^2\right) + \frac{108}{25} g_1^4 + 2\lambda_5[4\mathrm{Tr}(\mathbf{h}^\dagger\mathbf{h}) + T] - 8\mathrm{Tr}(\mathbf{Y}_\ell^\dagger\mathbf{Y}_\ell\mathbf{h}^\dagger\mathbf{h}); \\
16\pi^2 \frac{d\lambda_6}{dt} &= 4\lambda_2\lambda_6 + 4\lambda_3\lambda_6 + 4\lambda_4\lambda_5 + 4\lambda_6^2 - \frac{90}{5}\lambda_6 g_1^2 + \frac{432}{25} g_1^4 + 8\lambda_6[\mathrm{Tr}(\mathbf{f}^\dagger\mathbf{f}) + \mathrm{Tr}(\mathbf{h}^\dagger\mathbf{h})].
\end{aligned} \tag{C4}$$

The RGEs for the mass parameters are given by Eq. (4.9).

APPENDIX D: COMPLETE SET OF RGES FOR INERT DOUBLET MODEL

The one-loop RGEs for the inert doublet model have already been computed. The SM gauge coupling RGEs are given by

$$16\pi^2 \frac{dg_i}{dt} = b_i g_i^3, \tag{D1}$$

where $b_i = (-7, -3, \frac{21}{5})$ are the β-coefficients of the SM gauge couplings updated with the added particles.

The quark sector of the model remains unchanged, while the leptonic sector needs to be revisited. The RGEs for the leptonic Yukawa couplings are [33]

$$\begin{aligned}
16\pi^2 \frac{d\mathbf{Y_e}}{dt} &= \mathbf{Y_e}\left\{\frac{3}{2}\mathbf{Y_e^\dagger Y_e} + \frac{1}{2}\mathbf{h}^\dagger\mathbf{h} + T - \frac{9}{4} g_1^2 - \frac{9}{4} g_2^2\right\}; \\
16\pi^2 \frac{d\mathbf{h}}{dt} &= \mathbf{h}\left\{\frac{3}{2}\mathbf{h}^\dagger\mathbf{h} + \frac{1}{2}\mathbf{Y_e^\dagger Y_e} + T_\nu - \frac{9}{20} g_1^2 - \frac{9}{4} g_2^2\right\}; \\
16\pi^2 \frac{d\mathbf{M}}{dt} &= \{(\mathbf{h}\mathbf{h}^\dagger)\mathbf{M} + \mathbf{M}(\mathbf{h}\mathbf{h}^\dagger)^*\}.
\end{aligned} \tag{D2}$$

For the quartic scalar coupling we find the following set of RGEs [46]:

$$16\pi^2\frac{d\lambda_1}{dt} = 12\lambda_1^2 + 4\lambda_3^2 + 4\lambda_3\lambda_4 + 2\lambda_4^2 + 2\lambda_5^2 + \frac{3}{4}\left(\frac{9}{25}g_1^4 + \frac{6}{5}g_1^2g_2^2 + 3g_2^4\right) - 3\lambda_1\left(\frac{3}{5}g_1^2 + 3g_2^2\right) + 4\lambda_1 T - 4H;$$
$$16\pi^2\frac{d\lambda_2}{dt} = 12\lambda_2^2 + 4\lambda_3^2 + 4\lambda_3\lambda_4 + 2\lambda_4^2 + 2\lambda_5^2 + \frac{3}{4}\left(\frac{9}{25}g_1^4 + \frac{6}{5}g_1^2g_2^2 + 3g_2^4\right) - 3\lambda_2\left(\frac{3}{5}g_1^2 + 3g_2^2\right) + 4\lambda_2 T_\nu - 4T_{4\nu};$$
$$16\pi^2\frac{d\lambda_3}{dt} = 2(\lambda_1+\lambda_2)(3\lambda_3+\lambda_4) + 4\lambda_3^2 + 2\lambda_4^2 + 2\lambda_5^2 + \frac{3}{4}\left(\frac{9}{25}g_1^4 - \frac{6}{5}g_1^2g_2^2 + 3g_2^4\right) - 3\lambda_3\left(\frac{3}{5}g_1^2 + 3g_2^2\right) + 2\lambda_3(T+T_\nu) - 4T_{\nu e}; \tag{D3}$$

$$16\pi^2\frac{d\lambda_4}{dt} = 2(\lambda_1+\lambda_2)\lambda_4 + 8\lambda_3\lambda_4 + 4\lambda_4^2 + 8\lambda_5^2 + \frac{9}{5}g_1^2g_2^2 - 3\lambda_4\left(\frac{3}{5}g_1^2 + 3g_2^2\right) + 2\lambda_4(T+T_\nu) + 4T_{\nu e}; \tag{D4}$$

$$16\pi^2\frac{d\lambda_5}{dt} = \lambda_5\left[2(\lambda_1+\lambda_2) + 8\lambda_3 + 12\lambda_4 - 3\left(\frac{3}{5}g_1^2 + 3g_2^2\right) + 2(T+T_\nu)\right];$$
$$\text{where } T_\nu \equiv \mathrm{Tr}[\mathbf{h}^\dagger\mathbf{h}]; \qquad T_{4\nu} \equiv \mathrm{Tr}[\mathbf{h}^\dagger\mathbf{h}\mathbf{h}^\dagger\mathbf{h}]; \qquad T_{\nu e} \equiv \mathrm{Tr}[\mathbf{h}^\dagger\mathbf{h}\mathbf{Y}_\mathbf{e}^\dagger\mathbf{Y}_\mathbf{e}]. \tag{D5}$$

The RGEs for the mass parameters are given by Eq. (5.5). One notices from the set of RGEs that the evolution of the Majorana mass ($\mathbf{M}$), the new Yukawa coupling ($\mathbf{h}$), and the scalar quartic coupling λ_5 are proportional to the respective quantities themselves. The upshot of this setting is that these parameters remain small if they are small at any energy scale. This feature of the model becomes self-explanatory upon realization that if any of these parameters becomes zero, the neutrino becomes massless and global $U(1)$ symmetry conserving the lepton number is restored.

APPENDIX E: COMPLETE SET OF RGES FOR SCALAR SINGLET DARK MATTER MODEL

While the RGEs for the mass parameters are given by Eq. (6.4), the RGEs for the quartic couplings are given by

$$16\pi^2\frac{d\lambda_1}{dt} = 12\lambda_1^2 - 3\lambda_1\left(\frac{3}{5}g_1^2 + 3g_2^2\right) + \frac{3}{2}g_2^4 + \frac{3}{4}\left(g_2^2 + \frac{3}{5}g_1^2\right)^2 + 4\lambda_1 T - 4H + \frac{\lambda_3^2}{2};$$
$$16\pi^2\frac{d\lambda_2}{dt} = 3\lambda_2^2 + \frac{4}{3}\lambda_3^2;$$
$$16\pi^2\frac{d\lambda_3}{dt} = 6\lambda_3(\lambda_1+\lambda_2). \tag{E1}$$

RGEs for the Yukawa couplings and the gauge couplings remain the same as the SM.

APPENDIX F: COMPLETE SET OF RGES FOR VECTORLIKE FERMION MODEL

The RGEs for the mass parameters are given by Eq. (7.8). The RGEs for the gauge couplings are given by

$$16\pi^2\frac{dg_i}{dt} = b_i g_i^3, \tag{F1}$$

where $b_i = \{-3, \frac{-19}{6}, \frac{105}{10}, \frac{259}{3}\}$.

The set of RGEs for all the Yukawa couplings is given by

$$
\begin{aligned}
16\pi^2\frac{d\mathbf{Y_u}}{dt} &= \mathbf{Y_u}\left[\frac{3}{2}(\mathbf{Y_u^\dagger Y_u}-\mathbf{Y_d^\dagger Y_d})+\frac{1}{2}\mathbf{G_u^\dagger G_u}+T-\frac{17}{20}g_1^2-\frac{9}{4}g_2^2-8g_3^2-3g_4^2\right];\\
16\pi^2\frac{d\mathbf{Y_d}}{dt} &= \mathbf{Y_d}\left[\frac{3}{2}(\mathbf{Y_d^\dagger Y_d}-\mathbf{Y_u^\dagger Y_u})+\frac{1}{2}\mathbf{G_d^\dagger G_d}+T-\frac{1}{4}g_1^2-\frac{9}{4}g_2^2-8g_3^2-3g_4^2\right];\\
16\pi^2\frac{d\mathbf{Y_e}}{dt} &= \mathbf{Y_e}\left[\frac{3}{2}\mathbf{Y_e^\dagger Y_e}+\frac{1}{2}\mathbf{G_e^\dagger G_e}+T-\frac{9}{4}g_1^2-\frac{9}{4}g_2^2-3g_4^2\right];\\
16\pi^2\frac{d\mathbf{F_u}}{dt} &= \mathbf{F_u}\left[\mathbf{F_u^\dagger F_u}+T_F-\frac{8}{5}g_1^2-8g_3^2-15g_4^2\right]+\frac{1}{2}\mathbf{G_u G_u^\dagger F_u};\\
16\pi^2\frac{d\mathbf{F_d}}{dt} &= \mathbf{F_d}\left[\mathbf{F_d^\dagger F_d}+T_F-\frac{2}{5}g_1^2-8g_3^2-15g_4^2\right]+\frac{1}{2}\mathbf{G_d G_d^\dagger F_d};\\
16\pi^2\frac{d\mathbf{F_e}}{dt} &= \mathbf{F_e}\left[\mathbf{F_e^\dagger F_e}+T_F-\frac{18}{5}g_1^2-15g_4^2\right]+\frac{1}{2}\mathbf{G_e G_e^\dagger F_e};\\
16\pi^2\frac{d\mathbf{G_u}}{dt} &= \mathbf{G_u}\left[\mathbf{G_u^\dagger G_u}+\mathbf{Y_u^\dagger Y_u}+T_G-\frac{8}{5}g_1^2-8g_3^2-6g_4^2\right]+\frac{1}{2}\mathbf{F_u F_u^\dagger G_u};\\
16\pi^2\frac{d\mathbf{G_d}}{dt} &= \mathbf{G_d}\left[\mathbf{G_d^\dagger G_d}+\mathbf{Y_d^\dagger Y_d}+T_G-\frac{2}{5}g_1^2-8g_3^2-6g_4^2\right]+\frac{1}{2}\mathbf{F_d F_d^\dagger G_d};\\
16\pi^2\frac{d\mathbf{G_e}}{dt} &= \mathbf{G_e}\left[\mathbf{G_e^\dagger G_e}+\mathbf{Y_e^\dagger Y_e}+T_G-\frac{18}{5}g_1^2-6g_4^2\right]+\frac{1}{2}\mathbf{F_e F_e^\dagger G_e}.
\end{aligned}
\tag{F2}
$$

The RGEs for scalar quartic couplings are given by

$$
\begin{aligned}
16\pi^2\frac{d\lambda_1}{dt} &= 12\lambda_1^2+2\lambda_4^2+2\lambda_5^2-3\lambda_1\left(\frac{3}{5}g_1^2+3g_2^2+4g_4^2\right)+\left(\frac{27}{100}g_1^4+\frac{9}{4}g_2^4+\frac{9}{10}g_1^2g_2^2\right)\\
&\quad+12g_4^2+6g_2^2g_4^2+\frac{18}{5}g_1^2g_4^2+4\lambda_1T-4H;\\
16\pi^2\frac{d\lambda_2}{dt} &= 10\lambda_2^2+4\lambda_4^2+2\lambda_6^2-12\lambda_2g_4^2+12g_4^4+\lambda_2T_F-4H_F;\\
16\pi^2\frac{d\lambda_3}{dt} &= 10\lambda_3^2+4\lambda_5^2+2\lambda_6^2-48\lambda_3g_4^2+48g_4^4+4\lambda_3T_G-4H_G;\\
16\pi^2\frac{d\lambda_4}{dt} &= 6\lambda_1\lambda_4+2\lambda_2\lambda_4+2\lambda_5\lambda_6+4\lambda_4^2-\lambda_4\left(\frac{9}{2}g_2^2+\frac{9}{10}g_1^2+12g_4^2\right)+12g_4^4+2\lambda_4(T+T_F);
\end{aligned}
\tag{F3}
$$

$$
\begin{aligned}
16\pi^2\frac{d\lambda_5}{dt} &= 6\lambda_1\lambda_5+4\lambda_3\lambda_5+2\lambda_4\lambda_6+4\lambda_5^2-\lambda_5\left(\frac{9}{2}g_2^2+\frac{9}{10}g_1^2+30g_4^2\right)+48g_4^4+2\lambda_5(T+T_G)-4H_{YG};\\
16\pi^2\frac{d\lambda_6}{dt} &= 4\lambda_2\lambda_6+4\lambda_3\lambda_6+4\lambda_4\lambda_5+4\lambda_6^2-30\lambda_6g_4^2+48g_4^4+2\lambda_6(T_F+T_G)-4H_{FG};
\end{aligned}
\tag{F4}
$$

where

$$
\begin{aligned}
T &= \mathrm{Tr}[\mathbf{Y_e^\dagger Y_e}+3\mathbf{Y_d^\dagger Y_d}+3\mathbf{Y_u^\dagger Y_u}];\\
T_F &= \mathrm{Tr}[\mathbf{F_e^\dagger F_e}+3\mathbf{F_d^\dagger F_d}+3\mathbf{F_u^\dagger F_u}];\\
T_G &= \mathrm{Tr}[\mathbf{G_e^\dagger G_e}+3\mathbf{G_d^\dagger G_d}+3\mathbf{G_u^\dagger G_u}];\\
H &= \mathrm{Tr}[\mathbf{Y_e^\dagger Y_e Y_e^\dagger Y_e}+3\mathbf{Y_d^\dagger Y_d Y_d^\dagger Y_d}+3\mathbf{Y_u^\dagger Y_u Y_u^\dagger Y_u}];\\
H_F &= \mathrm{Tr}[\mathbf{F_e^\dagger F_e F_e^\dagger F_e}+3\mathbf{F_d^\dagger F_d F_d^\dagger F_d}+3\mathbf{F_u^\dagger F_u F_u^\dagger F_u}];\\
H_G &= \mathrm{Tr}[\mathbf{G_e^\dagger G_e G_e^\dagger G_e}+3\mathbf{G_d^\dagger G_d G_d^\dagger G_d}+3\mathbf{G_u^\dagger G_u G_u^\dagger G_u}];\\
H_{YG} &= \mathrm{Tr}[\mathbf{Y_e^\dagger Y_e G_e^\dagger G_e}+3\mathbf{Y_d^\dagger Y_d G_d^\dagger G_d}+3\mathbf{Y_u^\dagger Y_u G_u^\dagger G_u}];\\
H_{FG} &= \mathrm{Tr}[\mathbf{F_e^\dagger F_e G_e^\dagger G_e}+3\mathbf{F_d^\dagger F_d G_d^\dagger G_d}+3\mathbf{F_u^\dagger F_u G_u^\dagger G_u}].
\end{aligned}
\tag{F5}
$$

[1] S. Chatrchyan *et al.* (CMS Collaboration), Phys. Lett. B **716**, 30 (2012); G. Aad *et al.* (ATLAS Collaboration), Phys. Lett. B **716**, 1 (2012).

[2] G. Aad *et al.* (ATLAS and CMS Collaborations), Phys. Rev. Lett. **114**, 191803 (2015).

[3] P. Minkowski, Phys. Lett. **67B**, 421 (1977); T. Yanagida, *Proceedings of the Workshop on Unified Theories and Baryon Number in the Universe, Tsukuba, 1979*, edited by A. Sawada and A. Sugamoto (KEK, Tsukuba, 1979); S. Glashow, in *Proceedings of Cargese 1979, Quarks and Leptons* (Plenum Press, New York, 1979); M. Gell-Mann, P. Ramond, and R. Slansky, Conf. Proc. **C790927**, 315 (1979); R. N. Mohapatra and G. Senjanovic, Phys. Rev. Lett. **44**, 912 (1980).

[4] J. Schechter and J. W. F. Valle, Phys. Rev. D **22**, 2227 (1980); G. Lazarides, Q. Shafi, and C. Wetterich, Nucl. Phys. **B181**, 287 (1981); R. N. Mohapatra and G. Senjanovic, Phys. Rev. D **23**, 165 (1981); C. Wetterich, Nucl. Phys. **B187**, 343 (1981); J. Schechter and J. W. F. Valle, Phys. Rev. D **25**, 774 (1982).

[5] A. Zee, Phys. Lett. **93B**, 389 (1980); **95B**, 461(E) (1980).

[6] K. S. Babu, Phys. Lett. B **203**, 132 (1988).

[7] G. R. Farrar and P. Fayet, Phys. Lett. **76B**, 575 (1978).

[8] H. C. Cheng, K. T. Matchev, and M. Schmaltz, Phys. Rev. D **66**, 036005 (2002).

[9] H. C. Cheng and I. Low, J. High Energy Phys. 09 (2003) 051; J. High Energy Phys. 08 (2004) 061; I. Low, J. High Energy Phys. 10 (2004) 067.

[10] N. G. Deshpande and E. Ma, Phys. Rev. D **18**, 2574 (1978).

[11] E. Ma, Phys. Rev. D **73**, 077301 (2006).

[12] T. W. B. Kibble, G. Lazarides, and Q. Shafi, Phys. Lett. **113B**, 237 (1982); R. N. Mohapatra, Phys. Rev. D **34**, 3457 (1986); A. Font, L. E. Ibanez, and F. Quevedo, Phys. Lett. B **228**, 79 (1989); L. M. Krauss and F. Wilczek, Phys. Rev. Lett. **62**, 1221 (1989); L. E. Ibanez and G. G. Ross, Phys. Lett. B **260**, 291 (1991); Nucl. Phys. **B368**, 3 (1992); S. P. Martin, Phys. Rev. D **46**, R2769 (1992).

[13] L. E. Ibanez and G. G. Ross, Phys. Lett. **110B**, 215 (1982); K. Inoue, A. Kakuto, H. Komatsu, and S. Takeshita, Prog. Theor. Phys. **68**, 927 (1982); **70**, 330(E) (1983); L. E. Ibanez, Phys. Lett. **118B**, 73 (1982); J. R. Ellis, D. V. Nanopoulos, and K. Tamvakis, Phys. Lett. **121B**, 123 (1983); J. R. Ellis, J. S. Hagelin, D. V. Nanopoulos, and K. Tamvakis, Phys. Lett. **125B**, 275 (1983); L. Alvarez-Gaume, J. Polchinski, and M. B. Wise, Nucl. Phys. **B221**, 495 (1983).

[14] A. de Rujula, H. Georgi, and S. L. Glashow, in *Fifth Workshop on Grand Unification*, edited by K. Kang, H. Fried, and P. Frampton (World Scientific, Singapore, 1984), p. 88; For an earlier discussion, see Y. Achiman and B. Stech, in *New Phenomena in Lepton-Hadron Physics*, edited by D. E. C. Fries and J. Wess (Plenum, New York, 1979), p. 303.

[15] K. S. Babu, X. G. He, and S. Pakvasa, Phys. Rev. D **33**, 763 (1986); G. M. Pelaggi, A. Strumia, and S. Vignali, J. High Energy Phys. 08 (2015) 130.

[16] J. E. Camargo-Molina, A. P. Morais, R. Pasechnik, and J. Wessn, J. High Energy Phys. 09 (2016) 129.

[17] K. S. Babu, B. Bajc, and S. Saad, Phys. Rev. D **94**, 015030 (2016).

[18] K. S. Babu, I. Gogoladze, P. Nath, and R. M. Syed, Phys. Rev. D **72**, 095011 (2005).

[19] For example: C. Englert, J. Jaeckel, V. V. Khoze, and M. Spannowsky, J. High Energy Phys. 04 (2013) 060; A. Salvio and A. Strumia, J. High Energy Phys. 06 (2014) 080; A. D. Plascencia, J. High Energy Phys. 09 (2015) 026.

[20] S. R. Coleman and E. J. Weinberg, Phys. Rev. D **7**, 1888 (1973).

[21] H. Arason, D. J. Castano, B. Keszthelyi, S. Mikaelian, E. J. Piard, P. Ramond, and B. D. Wright, Phys. Rev. D **46**, 3945 (1992); M. x. Luo and Y. Xiao, Phys. Rev. Lett. **90**, 011601 (2003).

[22] F. Vissani, Phys. Rev. D **57**, 7027 (1998).

[23] A. Arhrib, R. Benbrik, M. Chabab, G. Moultaka, M. C. Peyranere, L. Rahili, and J. Ramadan, Phys. Rev. D **84**, 095005 (2011).

[24] M. A. Schmidt, Phys. Rev. D **76**, 073010 (2007); **85**, 099903(E) (2012).

[25] M. Farina, D. Pappadopulo, and A. Strumia, J. High Energy Phys. 08 (2013) 022.

[26] I. Gogoladze, N. Okada, and Q. Shafi, Phys. Rev. D **78**, 085005 (2008); A. Kobakhidze and A. Spencer-Smith, J. High Energy Phys. 08 (2013) 036.

[27] K. S. Babu and J. Julio, AIP Conf. Proc. **1604**, 134 (2014).

[28] K. S. Babu and C. Macesanu, Phys. Rev. D **67**, 073010 (2003).

[29] M. Nebot, J. F. Oliver, D. Palao, and A. Santamaria, Phys. Rev. D **77**, 093013 (2008); J. Herrero-Garcia, M. Nebot, N. Rius, and A. Santamaria, Nucl. Phys. **B885**, 542 (2014); D. Schmidt, T. Schwetz, and H. Zhang, Nucl. Phys. **B885**, 524 (2014); J. Herrero-Garcia, M. Nebot, N. Rius, and A. Santamaria, Nucl. Part. Phys. Proc. **273–275**, 1678 (2016).

[30] R. Barbieri, L. J. Hall, and V. S. Rychkov, Phys. Rev. D **74**, 015007 (2006); J. A. Casas, J. R. Espinosa, and I. Hidalgo, Nucl. Phys. **B777**, 226 (2007).

[31] E. Ma, Mod. Phys. Lett. A **21**, 1777 (2006).

[32] T. Hambye and M. H. G. Tytgat, Phys. Lett. B **659**, 651 (2008).

[33] A. Merle and M. Platscher, Phys. Rev. D **92**, 095002 (2015).

[34] V. Silveira and A. Zee, Phys. Lett. **161B**, 136 (1985); J. McDonald, Phys. Rev. D **50**, 3637 (1994).

[35] M. Kadastik, K. Kannike, and M. Raidal, Phys. Rev. D **80**, 085020 (2009); **81**, 029903(E) (2010); Y. Mambrini, N. Nagata, K. A. Olive, and J. Zheng, Phys. Rev. D **93**, 111703 (2016).

[36] K. S. Babu and R. N. Mohapatra, Phys. Rev. Lett. **62**, 1079 (1989).

[37] K. S. Babu and R. N. Mohapatra, Phys. Rev. D **41**, 1286 (1990).

[38] R. N. Mohapatra and Y. Zhang, J. High Energy Phys. 06 (2014) 072.

[39] P. S. B. Dev, R. N. Mohapatra, and Y. Zhang, J. High Energy Phys. 02 (2016) 186.

[40] S. M. Barr, Phys. Rev. Lett. **53**, 329 (1984); A. E. Nelson, Phys. Lett. **136B**, 387 (1984).

[41] CMS Collaboration, Report No. CMS-PAS-EXO-15-004; ATLAS Collaboration, Report No. ATLAS-CONF-2015-081;

M. Aaboud *et al.* (ATLAS Collaboration), J. High Energy Phys. 09 (2016) 001; V. Khachatryan *et al.* (CMS Collaboration), Phys. Rev. Lett. **117**, 051802 (2016).
[42] CMS Collaboration, Report No. CMS-PAS-EXO-16-027; ATLAS Collaboration, Report No. ATLAS-CONF-2016-059.
[43] K. P. Hadeler, Linear Algebra Appl. **49**, 79 (1983).
[44] K. G. Klimenko, Theor. Math. Phys. **62**, 58 (1985).
[45] W. Chao, J. H. Zhang, and Y. Zhang, J. High Energy Phys. 06 (2013) 039.
[46] C. T. Hill, C. N. Leung, and S. Rao, Nucl. Phys. **B262**, 517 (1985).